CDF/ANAL/BOTTOM/CDFR/7434

Characterization of the $B_c \to J/\psi\ \pi^+$ candidates and evidence for partially reconstructed decays $B_c \to J/\psi+$ *track* + X

P. Bussey, S. D'Auria, L. Nicolas, V. Papadimitriou, M. Spezziga
Godparents: A. Wicklund, S. Levy, S. Menzemer

April 1, 2005

Abstract

We describe the characterization of the $B_c \to J/\psi\ \pi^+$ signal candidates and details of the calculation of the significance of the observed signal. We also describe a vertex-based search for partially reconstructed $B_c \to J/\psi+$*track* + X decays made by relaxing the pointing cuts and the χ^2 cuts. In the region $5.6 < M(J/\psi\pi) < 6.187$ GeV/c^2 we observe an excess of $172 \pm 49_{stat} \pm 15_{sys}$ candidates that are characterized by a low impact parameter of a track with respect to a displaced J/ψ. This excess is interpreted as due to partially reconstructed decays of the B_c.

1 Introduction

This note is an accompaniment to the draft PRL paper and the previous notes[1, 2, 3, 4] describing the analysis of the CDF signal for $B_c \to J/\psi\,\pi$.

The search for the fully reconstructed decay $B_c \to J/\psi\ \pi$ signal followed a blind analysis procedure, the entire mass spectrum in the region 5.6 to 7.2 GeV/c^2 being blinded while the cut optimization was performed. The procedure to calculate the signal significance was then established and approved before "opening the box", and was subsequently followed precisely in un-blinding the mass plot. All this is described in [4]. We found a significant peak of 19 signal events with a background of 10 events, present in 360 pb^{-1} data. The associated mass value is $(6287.0 \pm 4.5 \pm 1.1)$ MeV/c^2.

In the present note we give further details of the 19 signal events, together with replies to some questions asked by the godparent committee and by other CDF collaborators. These include: questions concerning the "Toy Monte Carlo" method used to establish the threshold of the Significance Function (Score Function, Σ) that corresponds to a false signal probability of about 0.1%; issues concerning whether the track quality of the signal events differs from that of the background events; properties of the variables that were cut on; general candidate quality; physical properties of the lower sideband.

2 Detailed description of the toy Monte Carlo method

2.1 Distributions used in toy Monte Carlo

The toy Monte Carlo study generated many statistically independent "experiments" which, for the purpose of the signal search, contained only background. The background distribution was configured using the information that we could get from the data and from Monte Carlo. The background was assumed to be "combinatorial", i.e. generated by a random coincidence between particles in the event, and "physical", i.e. generated from incompletely reconstructed decays of B_c mesons.

To parameterize the combinatorial background, we used the distribution of the candidates reconstructed by selecting muon pairs in the sidebands of the J/ψ, where the mass of the two muons was constrained to the central value of the sideband where it would have been assigned in the data (fig. 39 in [4], p31). This is reproduced in fig. 1. The combinatorial background distribution used in our toy Monte Carlo is parameterized to be proportional to $6.8 - 0.723 * x$, where x is the mass in GeV. The number of entries in the combinatorial background was chosen randomly for each experiment, being generated out of a Gaussian distribution with mean value $\mu = 300$ and width $\sigma = 14.14$.

In searching for a narrow signal corresponding to the decay $B_c \to J/\psi\pi$, we take into account the fact of the previous observation of the B_c in its semileptonic decays. Even in the absence of a $J/\psi\pi$ signal, a contribution to the observed mass spectrum arising from partially reconstructed B_c decays is therefore to be expected. As shown in fig. 2, the partially reconstructed decays would give rise to a broad bump in the low mass region, which we parametrized as a broad Gaussian for the purpose of generating toy-Monte Carlo distributions. The number of entries in the physical background was also generated randomly, with a Gaussian with $\mu = 80$, $\sigma = 10$. The choice of this number was made by rescaling to a reasonable theoretical estimate of 20 signal events the fully reconstructed Monte Carlo sample obtained using BGenerator, where we have 120 entries in the feed-down region for 34 signal events after all cuts are applied, for a B_c mass of 6.4 GeV/c^2 and lifetime $\tau = 0.46$ ps). There is a substantial uncertainty on this number of 20. The bins of the toy mass distribution histogram were filled (in sequence) with the physical background and the combinatorial background using the Root *FillRandom* function. We call one "experiment" each outcome of a single histogram filling process. Of course, the histograms are reset to zero after the fitting.

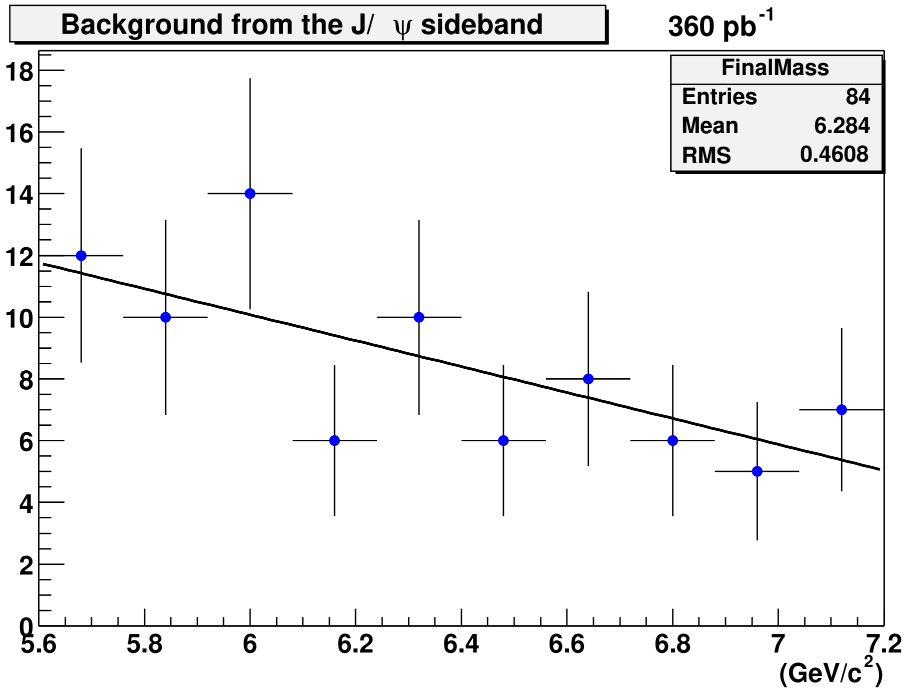

Figure 1: Background from data using the sidebands of the J/ψ mass peak and mass-constraining the J/ψ candidate tracks to the centre of the sideband where it belongs to. Re-binning has used in order to get fairly populated bins, for a binned fit. This figure has the same data as in fig. 39 of [4]

2.2 Fit used in toy Monte Carlo

As reported in [4], for fitting the toy Monte Carlo we used a Gaussian plus a linear background. The explicit formula used in the fit is:

$$f(x) = a + x\left(\frac{bw}{6\sigma m} - \frac{a}{m}\right) + \frac{wS}{\sigma\sqrt{2\pi}}\exp - \left(\frac{(x-m)^2}{2\sigma^2}\right) \quad (1)$$

where w is the bin width (w = 0.005), σ is the width of the Gaussian, x is its mass, and m is its mean value. S is the number of signal events, b is the number of background events within $\pm 3\sigma$ and a is the background constant.

The width (σ) of the Gaussian was fixed to: $\sigma = (3.95m - 9.37) * 0.001$ (GeV/c^2). This value was obtained from BGenerator Monte Carlo, by varying the mass of the generated B_c and

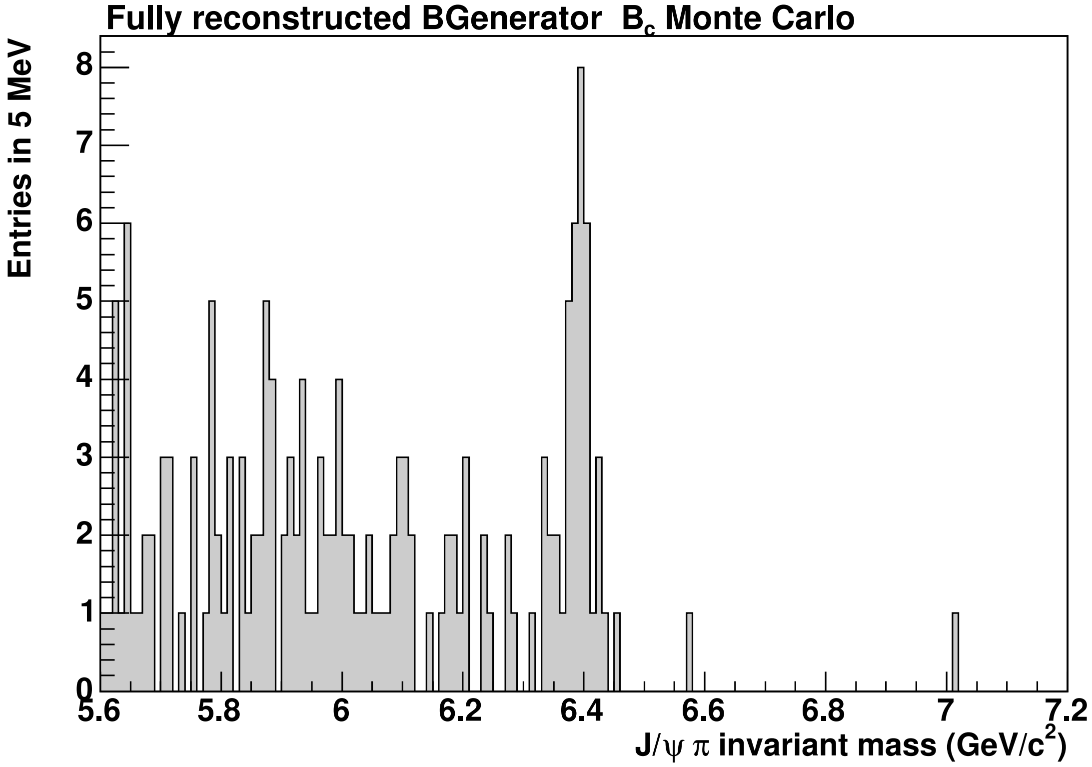

Figure 2: Invariant mass distribution obtained with a BGenerator Monte Carlo, where only B_c were generated according to the p_T spectrum (C) and assuming a lifetime of 0.46 ps and a mass M = 6.4 GeV/c^2. The decay table includes most decays to J/ψ but does not include the decays to $J/\psi\ a_1^+$ and hadronic decays to excited charmonium states. Events were fully simulated and reconstructed and all the analysis cuts have been applied.

fitting the width of the resulting signal after full reconstruction and analysis cuts. The mass (m) corresponding to the peak of the signal Gaussian was also fixed in each fit to a value that was incremented in 10 MeV steps ranging from 5.7 to 7.0 GeV/c^2. The number of events in the signal Gaussian (S) was constrained to lie in the range $0. < S < 100$. The fit range was from $m - 100$ to $m + 200$ MeV/c^2. At the beginning of each step, the number of signal events was re-initialized to 1. The background level within $\pm 3\sigma$ under the peak (B) and the background slope were fit parameters, free to float, and were not reset at each step.

We performed 1000 experiments (130,000 fits) and for each experiment the maximum value of $\Sigma = \frac{S}{1.5+\sqrt{B}}$ was recorded. The distribution of this variable was used to determine the threshold value that corresponded to a probability of 0.1% of occurring by chance; this value was found to be $\Sigma_{th} = 3.5$.

This probability of 0.1% for a false positive outcome was chosen (quite arbitrarily) a priori of any experiment, and denoted a value considered to be satisfactory for claiming “evidence”. We did not expect to have enough data for a higher significance, e.g. one that would be “five-sigma” observation, but still we had almost four times more data than in Run I, while the number of expected events could certainly allow for an evidence in a wide region of the parameter space.

Having fixed this a priori probability value, the purpose of the toy Monte Carlo experiments was to establish the threshold value of Σ that corresponded to it. We looked for the value Σ_{th} which had 99.9% of the events below it and 0.1% above it: in other words, the 99.9^{th} percentile point of the Σ distribution.

3 Search for signal

The procedure outlined in the note describing the blind analysis [4] has been applied to the data upon unblinding. Exactly the same fit procedure that was applied to the "toy" Monte Carlo mass distribution was also applied to the data. The result the scan is shown in fig. 3. There is only one main peak, at a mass of about 6290 MeV/c^2, that reaches $\Sigma = 3.6$. As our threshold was determined a priori to be $\Sigma_{th} = 3.5$, we deduced that the signal is significant and we followed the procedures to measure the mass.

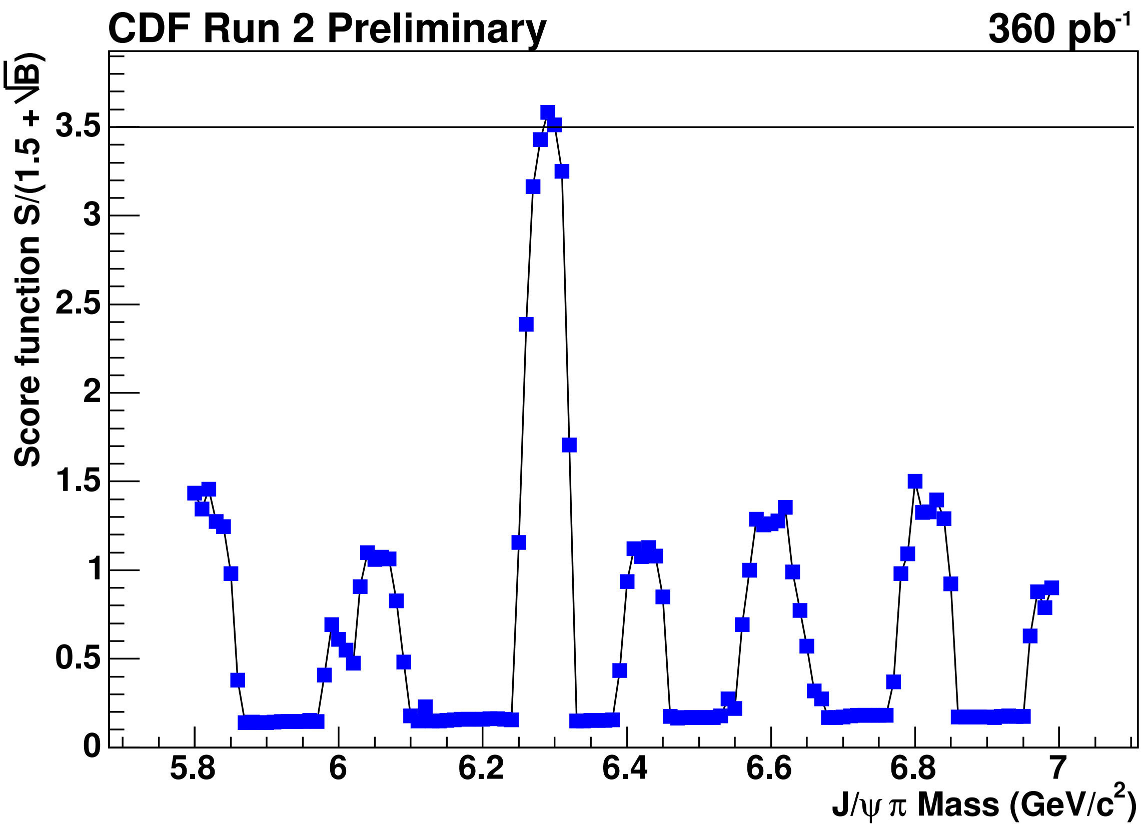

Figure 3: Result of the hypothesis test performed to establish the presence of a signal in the invariant mass distribution. Only one main peak is present and it passes the predetermined threshold of 3.5.

4 The invariant mass distribution

The invariant mass distribution for the whole search range after opening the box is shown in fig. 4. A peak is visible in the same position as indicated by the fit scan.

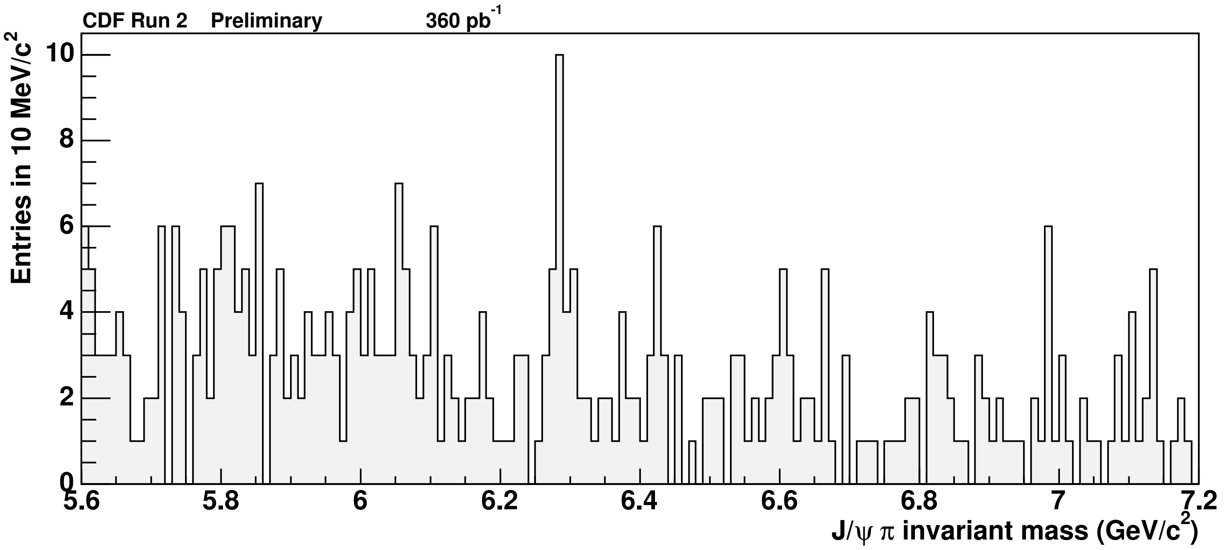

Figure 4: $J/\psi\ \pi$ invariant mass distribution, in the full search region.

Figure 5 shows the invariant mass distribution with a bin width of 10 MeV/c^2 in the range defined by $\pm 1\sigma$ of the Run I mass measurement.

We consider the region with $6.180 < M(J/\psi\pi) < 6.480$ that correspond approximatively to the fit window with the highest Σ value in fig 3 and we perform an unbinned likelihood fit. The templates are a gaussian, where the width is a linear function of the mass, and a linear background. The mass value is a fit parameter, together with the number of signal events, the number of background events and the background slope. The result is shown in fig. 6. We obtain 19 ± 6 signal candidates with a background of 10.0 ± 1.4.

The value of the mass is (6287.0 ± 4.8) MeV/c^2.

In the following we make use of the upper side band (USB), defined as the region $6.387 < M_{J/\psi\pi} < 7.200$ GeV/c^2 and the lower side band (LSB), defined as the region $5.8 < M_{J/\psi\pi} < 6.187$ GeV/c^2. The signal region comprises candidates with invariant mass $6.257 < M < 6.317$ GeV/c^2 fit . .

In the case of Monte Carlo, our sample had a B_c mass value set to 6.4 GeV/c^2; the same width of the lower sideband was adopted as in data, and the upper edge was set at the same distance from the mass value of the fully reconstructed decay.

The background in the data can be fitted with a broad Gaussian and a linear shape, and compared with the background assumed in the toy Monte Carlo studies (fig. 7, table 1). The distributions are in agreement within statistics.

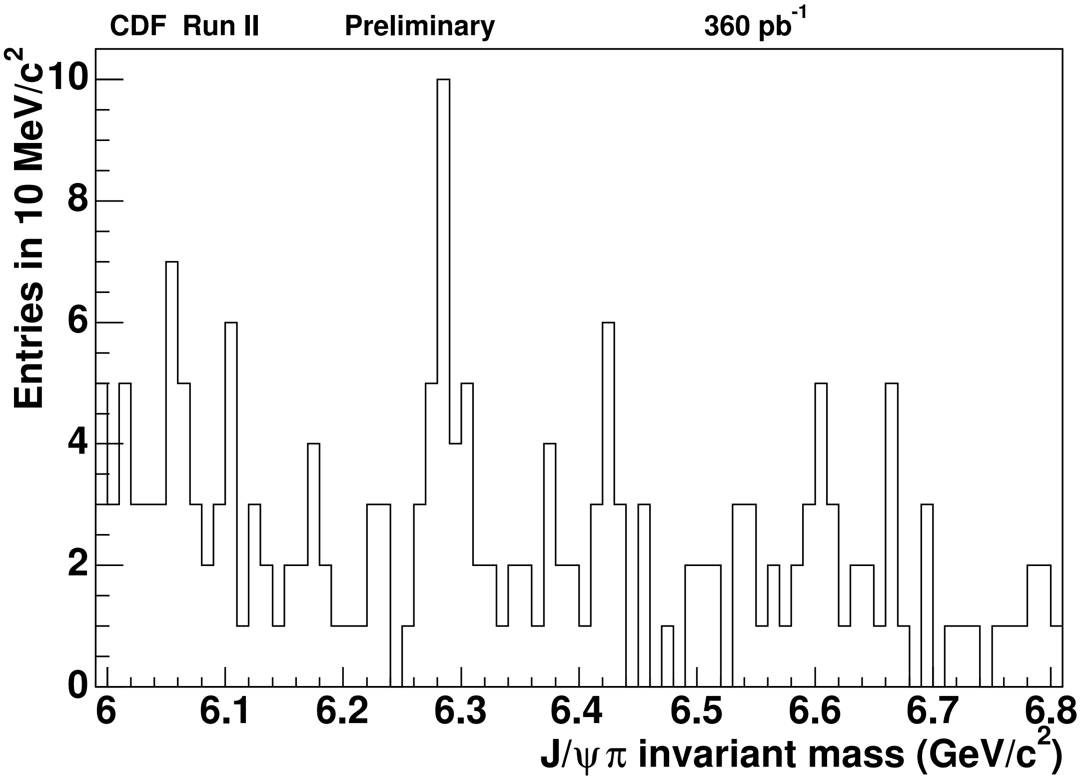

Figure 5: Distribution of the reconstructed $J/\psi\ \pi$ invariant mass, in the region 6.0 - 6.8 GeV/c^2.

5 Systematic uncertainty in the mass measurement

Most of the systematic uncertainties are taken from the cdf-note 6963 [13, 14, 15]. In order to be able to apply the systematic error analysis to our data we have performed an event-by-event comparison of the mass values for $B_u \rightarrow J/\psi K^+$ candidates that are in common in the two samples. We find 1166 common candidates. As shown in fig. 8 there is no bias between the two sets: the distribution of the event by event difference has a fit mean value at -5 keV. Note 6963 has used software rel/c^{2}ease 4.8.1 This analysis has used release 5.3.3. The mass resolution

Quantity	Toy MC	Fit to data
Events broad Gaussian	80	61 ± 38
Mass broad Gaussian (GeV/c^2)	5.80	5.87 ± 0.07
Width broad gaussian (MeV/c^2)	300	170 ± 75
Slope	-3.04	-0.10
Constant	29	36

Table 1: Comparison of the parameters used in the toy Monte Carlo with the parameters obtained from the fit to the data. The function describing the background is made of a linear part, modeling the combinatorial background, plus a broad gaussian, modeling the partially reconstructed decay modes.

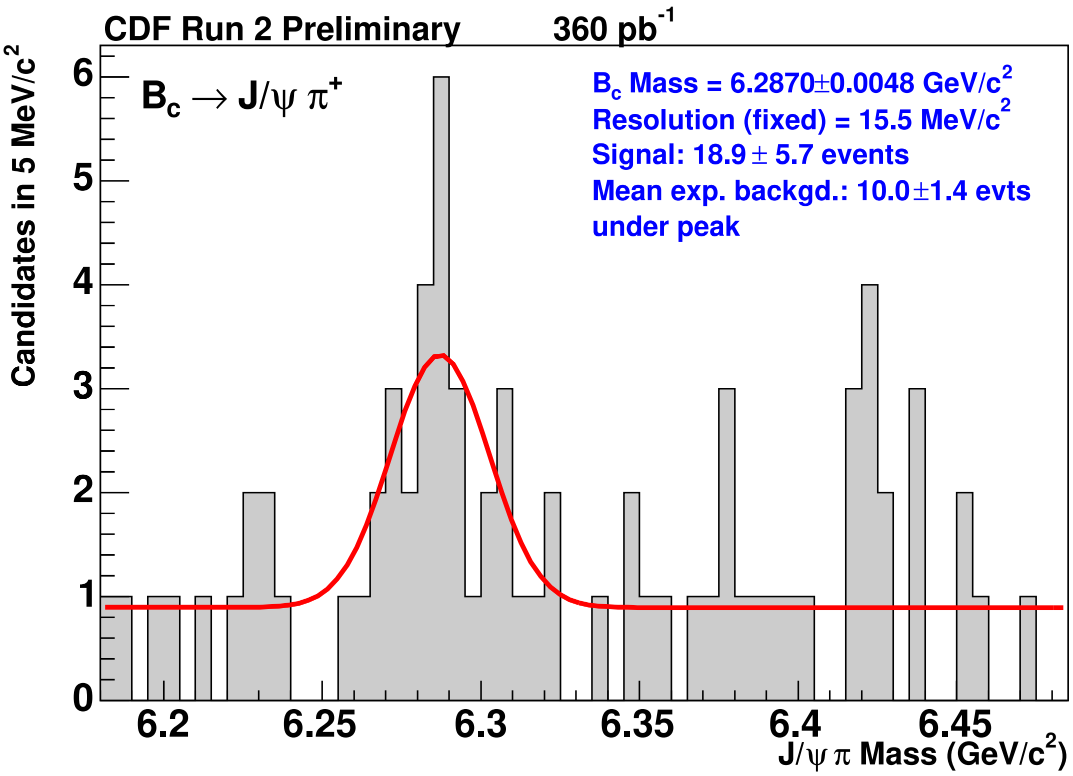

Figure 6: $J/\psi\ \pi$ invariant mass distribution, in the region indicated by the scan, with the result of unbinned likelihood fit to the mass and number of signal candidates. The background level and its slope were also fit parameters.

between the two releases has improved: e.g. the mass constrained $B_u \to J/\psi K^+$ signal resolution increased from 14.8 MeV/c^2 [14] to 11.5 MeV/c^2 [4]. we find that the distribution of the mass difference is a 2-component gaussian with widths $\sigma_a = 6.9$ MeV/c^2 and $\sigma_b = 15.6$ MeV/c^2. The weighted average is actually 10.9 MeV/c^2, in good agreement with the expected value obtained by subtracting in quadrature the two values reported above.

We take the tracking systematic error from [13, 14] as is. This takes into account the possible shift due to different types of tracks, as they can be detected by different tracking systems and algorithms. For the momentum scale we use table 12 of ref. [13] as a starting point: the Q-value of the decay $B_c \to J/\psi\pi^+$ is 3052 GeV/c^2. We take as a systematic error the full shift of 0.6 MeV/c^2.

A third source of systematic uncertainty is the different mass of the third track. This translates in the different probability of photon radiation and different energy loss. From table 14 of ref. [13] we estimate a possible effect of 0.2 MeV/c^2.

The momentum spectrum of the B_c meson is unknown. We find in B_u data a possible moderate effect of variation of the candidate mass as a function of its p_T, as shown in fig. 9. This effect is present in a much minor extent in Monte Carlo. Certainly, this effect is somehow correlated with the momentum scale. Software release 5.3.3 uses a different detector geometry description than release 4.8.1. In particular, the description of the material of the inner tracker is different [8]. Some additional systematic effect could have been hidden from [13] by the lower statistic and different

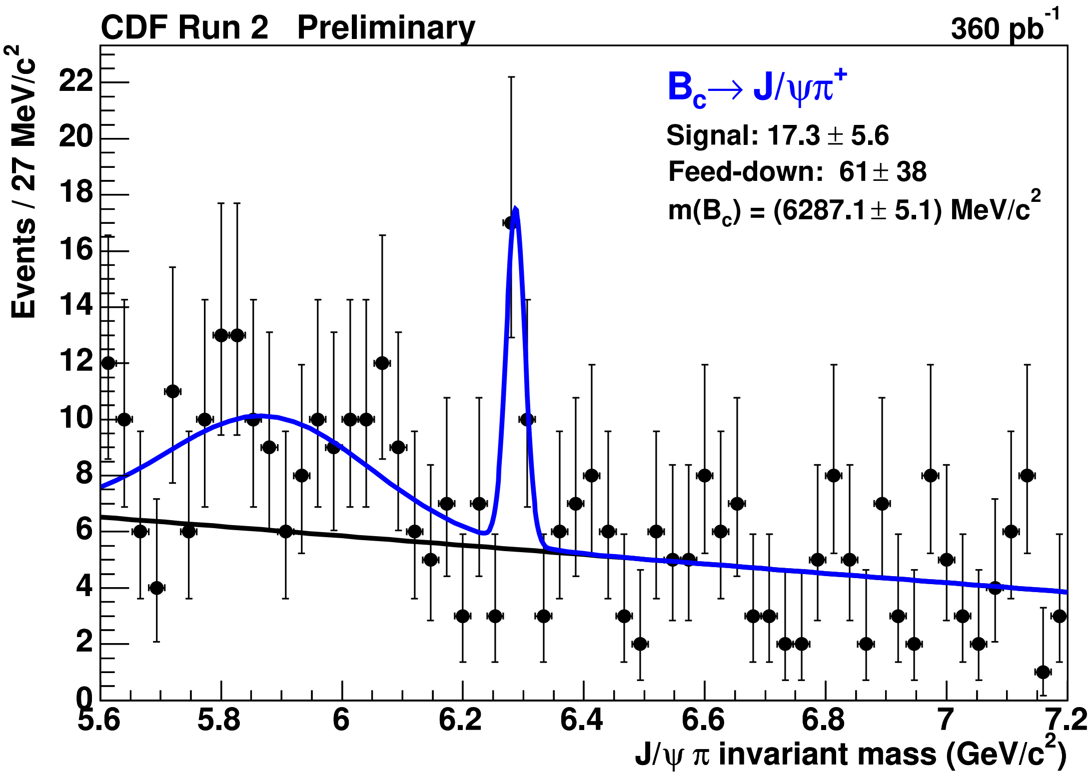

Figure 7: Unbinned likelihood fit to the mass distribution in the whole search region. The broad gaussian distribution describes the partially reconstructed decays to J/ψ + track + anything (feed-down), that constitutes our physical background

resolution. Based on fig. 9 we estimate, in a very conservative way, that the possible additional effect is 0.5 MeV/c^2.

The main contribution to the systematic uncertainty of the B_c mass comes from the parametrization of the background in the mass fit. The unbinned likelihood fit to the mass distribution that is reported in fig. 6 and constitutes our main result was limited to the region $6.180 < M(J/\psi\pi) < 6.480$ that corresponds to about 100 MeV/c^2 below and 200 MeV/c^2 above the peak. The background distribution was assumed to be linear in this interval, allowing for a slope which turned out to be negligible. The purpose of the limited and asymmetric range was to minimize the effect of the physical background on the peak position and on the number of candidates.

If we now fit the whole search range using the un-binned likelihood method (fig. 7) and defining the fit function as a narrow gaussian with width as a function of mass for the signal, a linear function for the combinatorial background and a broad gaussian for the Physical background we find a mass value that is up to 0.1 MeV/c^2 above the one obtained with the narrow fit region. Variations of 15% in the signal width also produce ≈ 0.2 MeV/c^2 variations in the mass value. Using the same fit function with a binned likelihood method (10 MeV/c^2 bins) we find a mass value that is 0.8 MeV/c^2 above. We take this value as a conservative estimate of the systematic error due to the fit procedure. The list of all systematic errors that are taken into account is reported in table 2.

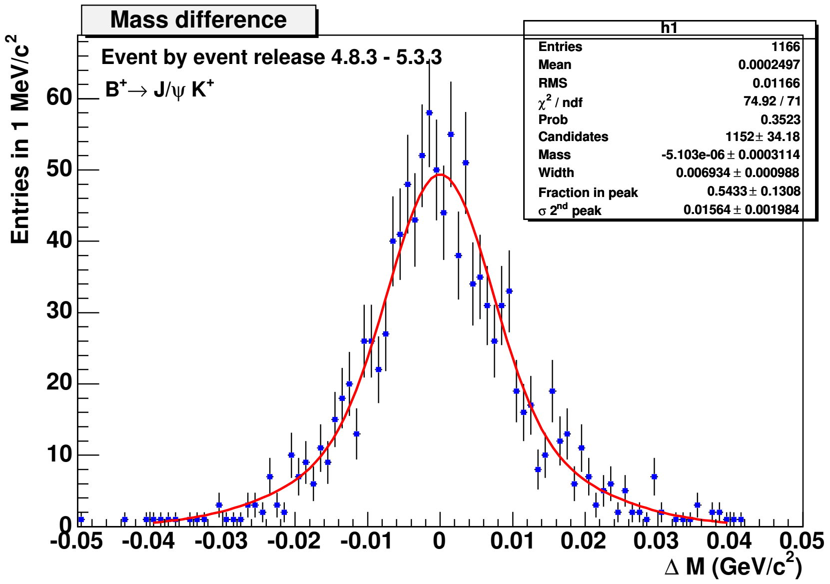

Figure 8: Event-by-event difference of the mass value for $B_u \to J/\psi K^+$ as measured in ref. [14] and in this work (and [4]). We find 1166 common candidates.

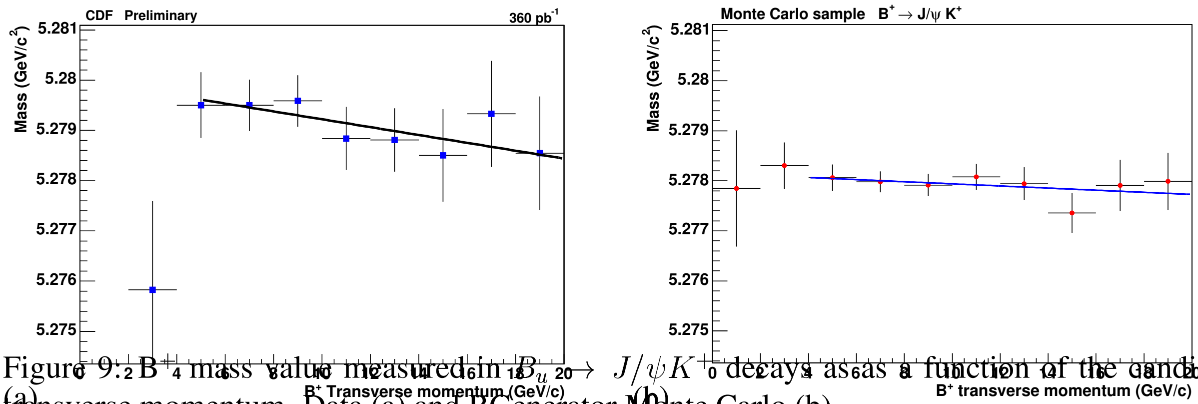

Figure 9: B+ mass value measured in $B_u \to J/\psi K^+$ decays as a function of the candidate transverse momentum. Data (a) and BGenerator Monte Carlo (b).

6 Track quality

In an assessment of the plausibility of a signal, the track quality for the events in the signal peak must be considered. The track quality for the entire sample of 390 events in the selected "blinded"

Source	MeV/c^2	Ref.
Momentum Scale	0.6	[15]
Tracking	0.2	[15]
π/K	0.2	
Δp_t	0.5	
Fit	0.8	
Total	1.1	

Table 2: Main systematic errors (in MeV/c^2) affecting the determination of B_c mass.

region was already assessed before unblinding [4]. Having obtained a signal, we now show plots to compare some relevant quality parameters of the events in the B_c signal region with those of the B_u events, which were used as a control sample. This control sample provides a more reliable experimental comparison than is obtained from the Monte Carlo samples. The signal region is defined in section 3 and all distributions are sideband subtracted.

Figures 10 - 12 show respectively the distributions of

- the number of SVX layers,
- the number of Layer 00 hits, and
- the number of silicon z hits per fitted track,

for three tracks per candidate, namely the two muons forming the J/ψ and the third track, taken as a pion in the B_c case and a kaon in the B_u case. In figures 10 and 12, the two distributions are the same within statistical errors. In fig. 11 there is a slight indication that the B_c candidates have more L00 hits than the B_u candidates.

Figures 13, 14 and 15 show the same distributions for just the third track. Fig. 15 shows the number of silicon layers with $90° z$-hits associated to the third track (pion or kaon). Figure. 16 shows the numbers of tracks having a L00 hit. Within statistics, the two distributions are similar.

In summary, we observe no statistically significant deviation of the B_c candidates from the B_u case. We conclude that the track quality of the B_c candidates is similar to that of the control sample, as regards these plotted parameters.

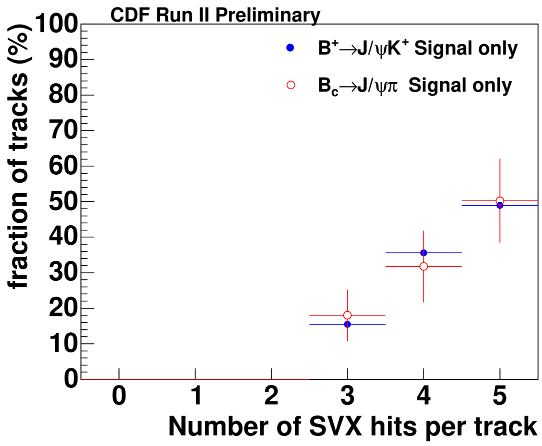

Figure 10: Fraction of tracks with SVX layers hit associated. A quality cut at 3 layers hit was used in both B_u and B_c case.

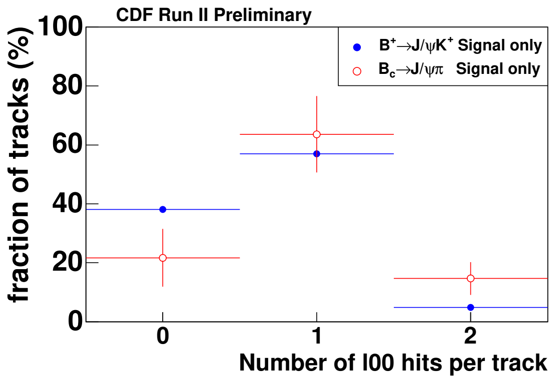

Figure 11: Fraction of tracks with L00 hits. Tracks with 2 hits cross overlapping silicon sensors.

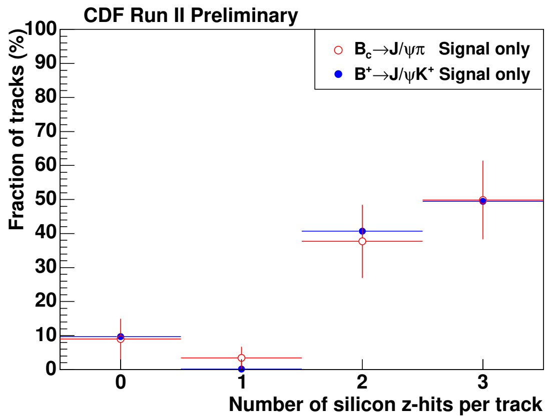

Figure 12: Fraction of tracks with silicon z-hits, all tracks in candidate.

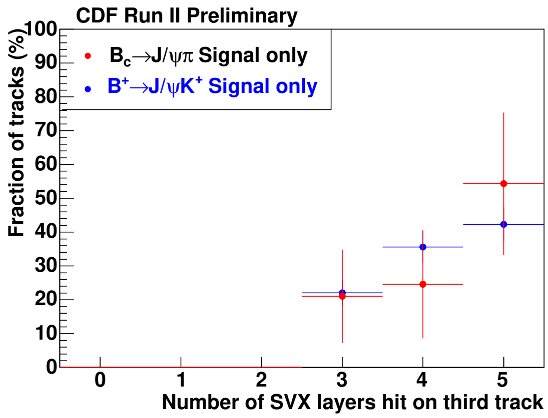

Figure 13: Fraction of third tracks with SVX layers hit associated. A quality cut at 3 layers hit was used in both B_u and B_c case.

7 Properties of the variables that were cut on.

In this section we consider the variables that were cut on; differences between the signal and background regions of the mass distribution are clearly to be expected. However the distributions

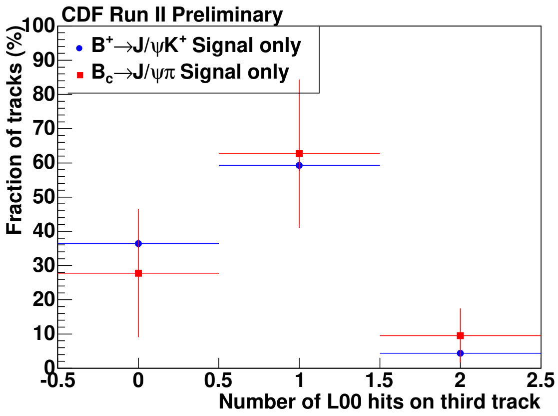

Figure 14: Fraction of third tracks with L00 hits. Tracks with 2 hits cross overlapping silicon sensors.

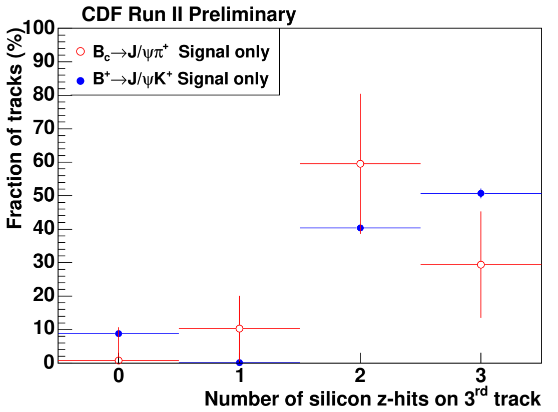

Figure 15: Fraction of tracks with silicon z-hits, only for *third tracks*.

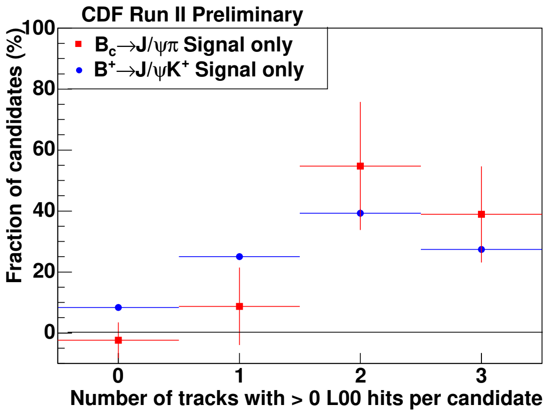

Figure 16: Distribution of the number of tracks with a L00 hit per candidate.

in the B_c signal region should, where appropriate, resemble those in the B_u control channel. Also, the distributions in the B_c signal region should look physically sensible. For these variables, a comparison is therefore presented between the data in the signal peak, the B_c Monte Carlo and the B_u control channel, which also has both data and Monte Carlo distributions. The plots are shown in fig. 17–23, in each case normalized to the number of B_c candidates. The starred points represent the background-subtracted B_c data in each case.

The following features are seen:

- 3-D vertex χ^2 distribution (fig. 17): the four distributions are similar below the cut value of 9.0.

- The third track contribution to the vertex χ^2 (fig. 18): the four distributions are similar below the cut value of 2.6.

- Impact parameter of the candidate (fig. 19): the four distributions are similar and centered on zero. It should be noted that the B_u has a longer lifetime than the B_c; the similarity of the distributions indicates that the uncertainty on the primary vertex position contributes significantly to the width of this plot. The cut value was 65μm.

- Pointing angle to the primary vertex in 3-D (fig. 20): the distributions are fairly similar below the cut value of 0.4 radians. This quantity is strongly correlated with that of fig 7. The shorter decay length of the B_c means that we would expect a larger error on this quantity for this particle.

- Pion/kaon p_T (fig. 21). There is no "pile-up" in the B_c distribution at the lower end, which might have indicated an excess of randomly associated soft tracks. The four plots are similar, within the low statistics. The cut value was 1.8 GeV/c.

- Significance of the measured decay length (fig. 22) In both cases the distribution is broad, and the B_c distribution shows no tendency to low or high values. The cut value was 4.4.

- Decay distance of candidates (fig. 23). The difference in lifetime of the two particles is very apparent. The B_c candidate distribution shows no features which appear anomalous. In this case the B_c signal has an upper cut at 650 μm, to exclude long-lived background, while there is not such a cut in the case of B_u.

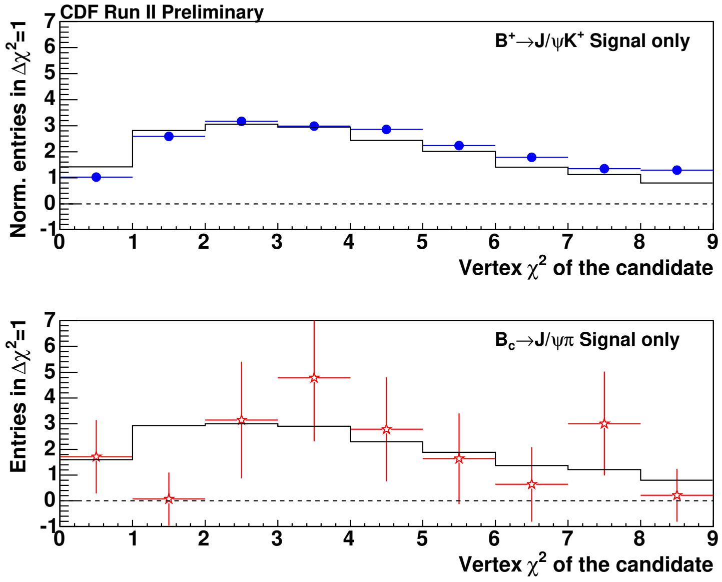

Figure 17: Vertex χ^2 in 3D. Upper plot: the χ^2 distribution for the B_u signal, sideband subtracted, superimposed on the same distribution for the BGenerator B_u Monte Carlo. Lower plot: the same distribution for the signal events, sideband subtracted (starred points). The histogram is the Monte Carlo distribution, from a BGenerator signal-only sample, with mass = 6.4 GeV/c^2 and $c\tau = 138\mu$m .

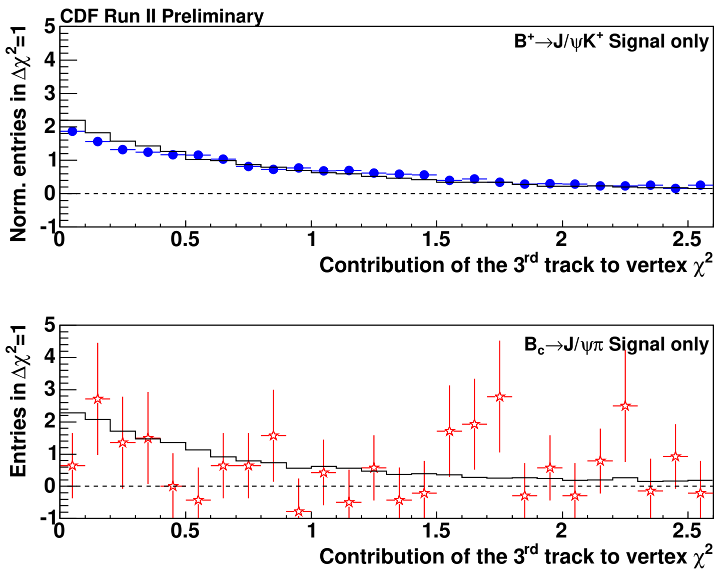

Figure 18: Contribution to the Vertex χ^2 from the third track. Upper plot: distribution for the B_u signal, sideband subtracted. Lower plot: the same distribution for our signal events, sideband subtracted (data points); the histogram shows the same distribution for candidates from the BGenerator Monte Carlo (signal-only sample), with mass = 6.4 GeV/c^2 and $c\tau = 138\mu$m.

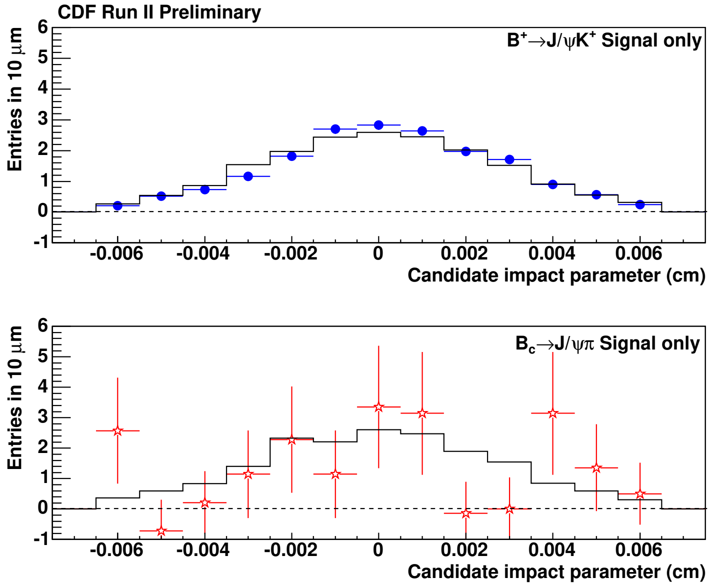

Figure 19: Candidate impact parameter with respect to the primary vertex. Upper plot: distribution for the B_u signal, sideband subtracted, superimposed on the same distribution for the BGenerator B_u Monte Carlo. Lower plot: the same distribution for the signal events, sideband subtracted (data points). The histogram in the lower plot is the same distribution for candidates from BGenerator Monte Carlo (signal-only sample), with mass = 6.4 GeV/c^2 and $c\tau = 138\mu$m.

8 General Candidate quality

We present here distributions for variables that were not used for cuts, but are however of general interest to characterize the signal. Some further comments are as follows:

- p_T of the candidate (fig. 24). The MC prediction for the B_c is model dependent and not identical to the distribution for the B_u. No B_c candidates were observed with $p_T < 4$ GeV/c, but there is a substantial contribution below 6.5 GeV/c. There is no pile-up in the B_c distribution and no evidence for anomalies.

- p_T of the J/ψ (fig. 25). The B_u, B_c and BGen distributions are all similar, with nothing anomalous seen. We note also in this case that there is substantial contribution at p_T as low as 1.5 GeV/c.

- Error on the transverse decay distance (fig. 26). The distribution has no anomalous peak at large values for the candidates; the B_c candidates have if anything smaller errors than the B_u candidates. This is attributable to the cut on the significance of L_{xy}: in the case of B_u the larger decay length allows events with a larger error on L_{xy} to pass the cuts.

- Decay topology (fig. 27). This indicates whether the third track emerged between the J/ψ tracks in the xy plane (internal) or outside (external). Randomly associated prompt tracks might be more likely to give internal candidates, while random tracks with impact parameter would be external. Nothing anomalous is seen in the comparison.

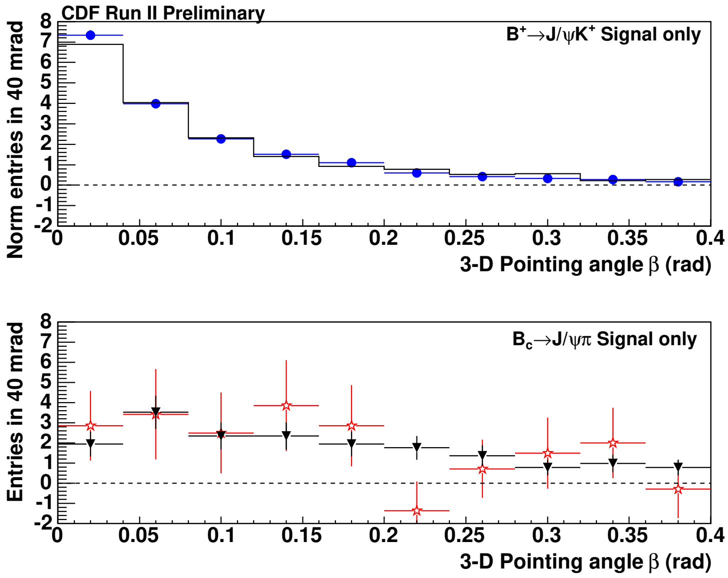

Figure 20: Pointing angle of the candidates, i.e. 3-D angle between the momentum and the direction of flight of the reconstructed candidate. Upper plot: distribution for the B_u signal, sideband subtracted, superimposed on the same distribution from the PYTHIA B_u Monte Carlo. Lower plot: the same distribution for the signal events, sideband subtracted (starred data points), with (triangles) the same distribution for candidates from PYTHIA, where the B_c meson has a mass = 6.4 GeV/c^2 and $c\tau = 138\mu$m.

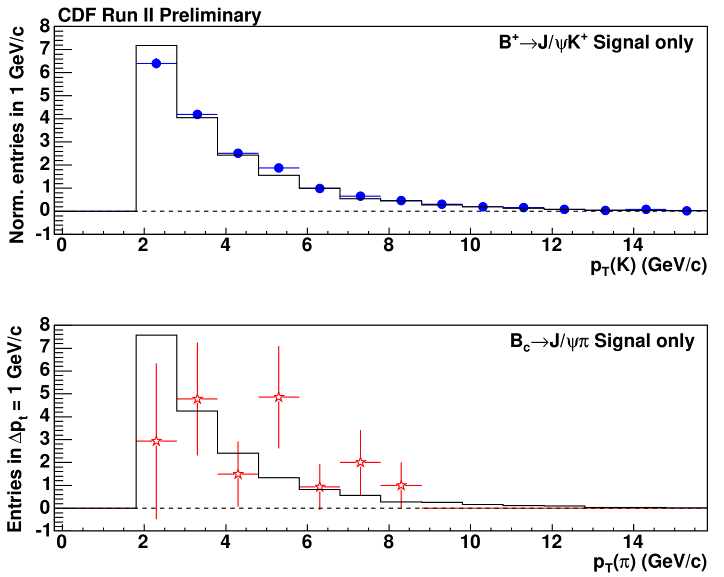

Figure 21: Value of p_T of the third track. Upper plot: distribution for the B_u signal, sideband subtracted. Lower plot: the same distribution for the signal events, sideband subtracted (data points). The histogram in the lower plot is the same distribution for candidates from BGenerator Monte Carlo (signal-only sample), with mass = 6.4 GeV/c^2 and $c\tau = 138\mu$m.

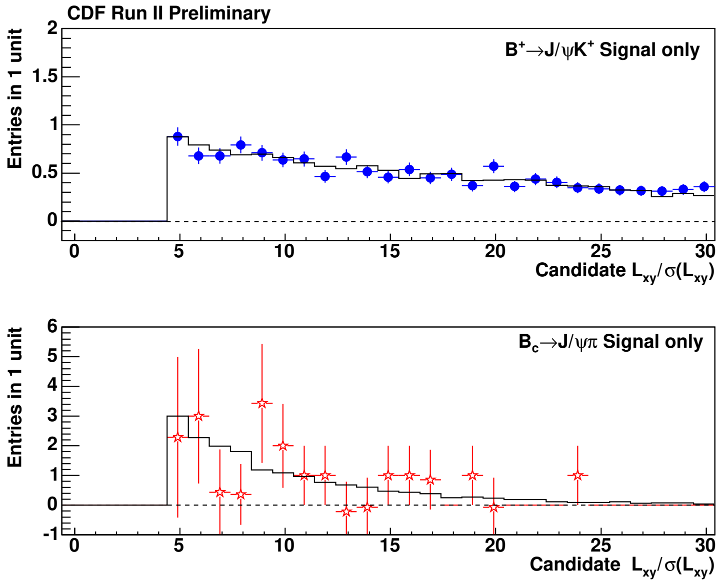

Figure 22: The L_{xy} significance. Upper plot: distribution for the B_u signal, sideband subtracted, superimposed on the same distribution for the BGenerator B_u Monte Carlo. Lower plot: the same distribution for the signal events, sideband subtracted (data points). The histogram in the lower plot is the same distribution for candidates from BGenerator Monte Carlo (signal-only sample), with mass = 6.4 GeV/c^2 and $c\tau = 138\mu$m. Note the different scale of the two plots.

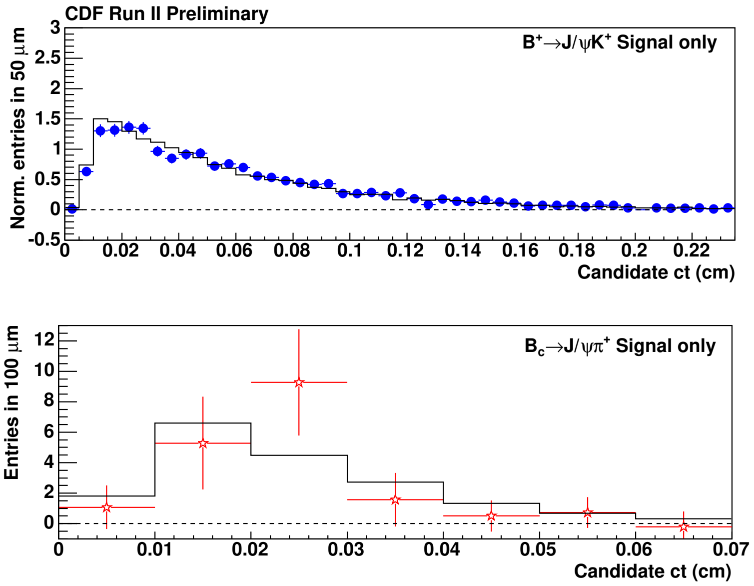

Figure 23: The ct of the candidates. Upper plot: distribution for the B_u signal, sideband subtracted, superimposed on the same distribution for the BGenerator B_u Monte Carlo. Lower plot: the same distribution for the signal events, sideband subtracted (data points). The histogram in the lower plot is the same distribution for candidates from BGenerator Monte Carlo (signal-only sample), with mass = 6.4 GeV/c^2 and $c\tau = 138\mu$m. Note the different ct scales.

– Pseudo-rapidity of the candidates (fig. 29). The B_c candidates appear to be more broadly distributed but in view of the sparse statistics it is difficult to draw any conclusions. There is no pile-up.

– Azimuthal angle of the candidates (fig. 30). Both the B_u and the B_c candidates show a broad distribution compatible with flatness. The shape due to the trigger coverage is also evident.

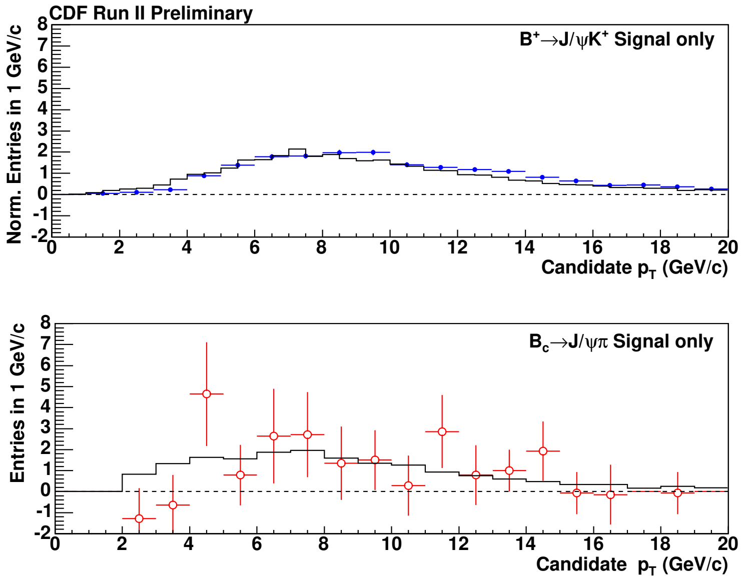

Figure 24: Distribution of the p_T of the candidates. Upper plot: the distribution for the B_u signal, sideband subtracted, compared with the distributions for Monte Carlo events. Lower plot: the same distribution for the signal events, sideband subtracted (data points). The histogram in the lower plot is the same distribution for candidates from BGenerator Monte Carlo (signal-only sample), with mass = 6.4 GeV/c^2 and $c\tau = 138\mu$m and p_T distribution from ref [9].

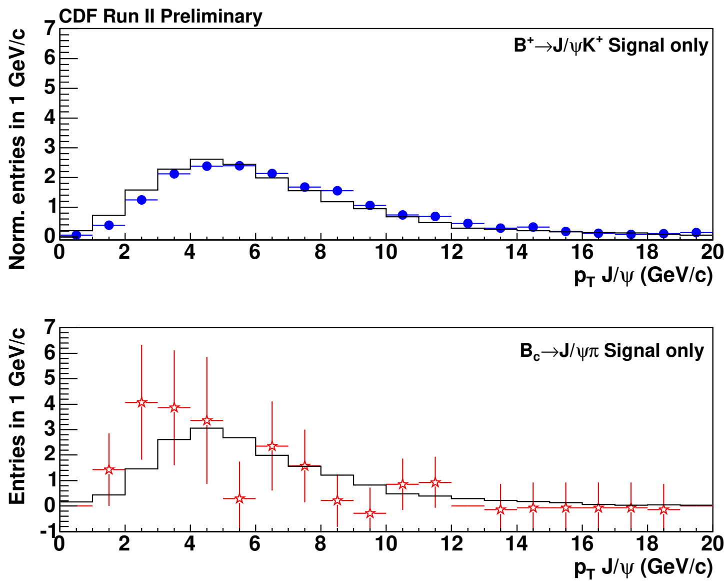

Figure 25: Distribution of the p_T of the J/ψ for candidates. Upper plot: the distribution for the J/ψ belonging to the B_u signal, sideband subtracted, compared with the distributions for Monte Carlo events. Lower plot: the same distribution for the signal events, sideband subtracted (data points). Lower plot: the same distribution for candidates from BGenerator Monte Carlo (signal-only sample), with mass = 6.4 GeV/c^2 and $c\tau = 138\mu$m and p_T distribution from ref [9].

9 A vertex-based analysis of the lower side band

It has been pointed out that the partially reconstructed decays $B_c \to J/\psi +$ *track* + *anything* are much more numerous than the exclusive decay that we are looking for and, therefore, their signature could be stronger than that of the signal. The partially reconstructed decays share with the signal the fact that at least three tracks originate from a common vertex. If the B_c mass is where the peak is, the partially reconstructed decays are expected to occur only in the lower sideband. In order to look for these "feed-down" candidates in the lower sideband region, we relax the cuts on the vertex χ^2 and on the pointing geometry (impact parameter and pointing angle). This allows more feed-down events to be accepted. In the hypothesis of a significant signal being present, the lower side band region will contain an excess of events with small impact parameter of the third track with respect to the vertex formed by the two muon tracks alone, namely the J/ψ vertex.

9.1 The control sample $B_{u,d} \to J/\psi + track + X$

We first check what is expected on the B_u control sample. In this case we expect contributions from both B^0 and B^+, where one or more hadron tracks are neglected, or one or more neutral hadrons are produced.

We relax the requirements to $\chi^2 < 50$, $d_0(B) < 2$ mm and 3-D pointing angle $\beta < \pi/2$, we apply no cut on the contribution to the vertex χ^2 from the third track and we leave the other cuts unchanged: p_T of the third track $p_T(\pi) \leq 1.8$ GeV/c and the significance of the 3-track projected decay length $\frac{L_{xy}}{\sigma(L_{xy})} < 4.4$ This set of cuts increases the B_u signal yield by a factor of 1.86 with

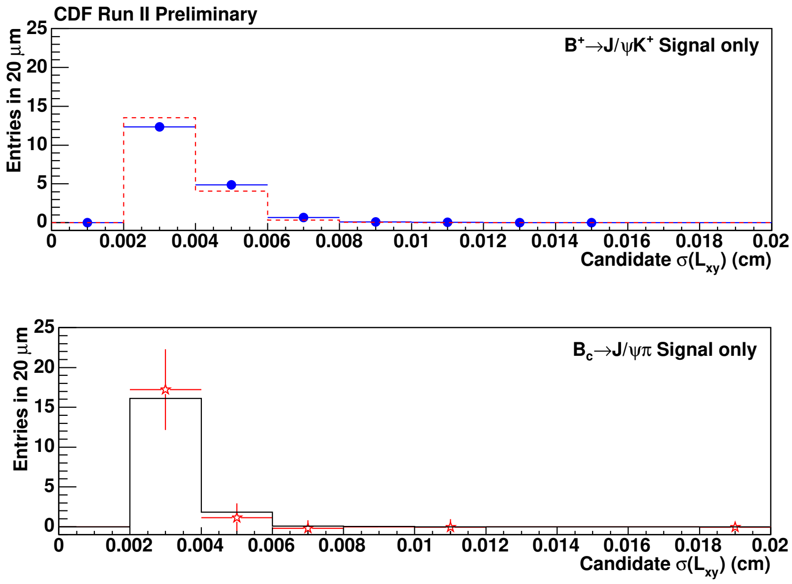

Figure 26: Distribution of the error on L_{xy}, as calculated by CTVMFT. Upper plot: the distribution for the B_u signal, sideband subtracted, the lower plot shows the same distribution for the signal events, sideband subtracted (data points). The histograms indicate the distributions for candidates from BGenerator Monte Carlo (signal-only samples). In the case of B_c we have used mass M = 6.4 GeV/c^2 and $c\tau = 138\mu$m. In the case of B_u a larger fraction of candidates with larger error can be accepted by our cuts, due to the larger lifetime (we cut on $L_{xy}/\sigma(L_{xy})$).

respect the cuts used in the analysis of the exclusive channel, giving (4416 ± 83) candidates (fig. 31) with relaxed cuts. As the decay topology is the same, we may expect about the same effect in case of the B_c. This means that the number of expected B_c signal events can normalized to 35 instead of 19.

Fig. 32 shows the impact parameter of the third track with respect to the J/ψ vertex (this impact parameter will be indicated with *i.p.*), as a function of the 3-track invariant mass, where the third track is assigned the K^+ mass and the muon pair is constrained to have the J/ψ invariant mass. The events are the same as those entering the mass spectrum in fig. 31. This distribution displays two well-distinguished regions, corresponding to the signal and to the feed-down of partially reconstructed decays, with a gap in between. The gap width is consistent with one pion mass, corresponding to a missing π^- in the case of B_d decays. With sideband definitions as shown in fig. 31, the slice projection distributions of the scatter plot are shown in fig. 33. The upper and lower sidebands (resp. USB and LSB) are defined as the following mass ranges: USB = [5.4, 5.7] and LSB = [4.9, 5.1] (GeV/c^2). As shown in fig. 33, both in the signal region and in the LSB a large population of candidates have a track consistent with originating from the same vertex as the J/ψ. In fig 34 we show the *i.p.* distribution for events in LSB and in the USB, where the USB distribution has been normalized to the same mass interval as the LSB. In fig. 35 we show the USB-subtracted *i.p.* distributions for both the signal (a) and the LSB (b) regions, with a fit to a double Gaussian shape, centered at zero. For the signal region we find $N_{u1} = 4422 \pm 81$ candidates, a narrow width $\sigma_1 = 28 \pm 2\mu$m (72% of candidates) and a wide width $\sigma_2 = 62 \pm 6\mu$m. This number of candidates is in very good agreement with what we obtain by fitting the mass distribution (fig. 31), which is

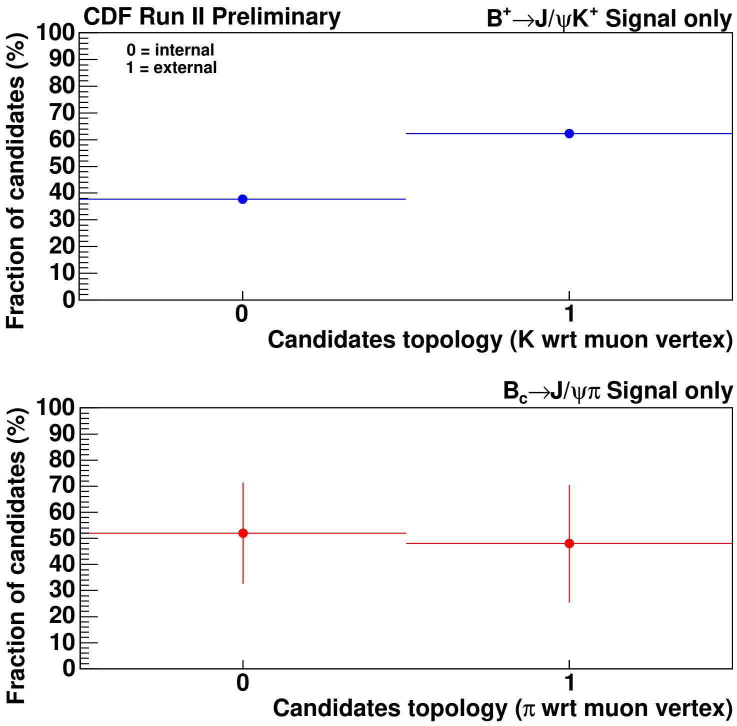

Figure 27: Topology of the vertex: internal or external third track w.r.t. the J/ψ candidate tracks.

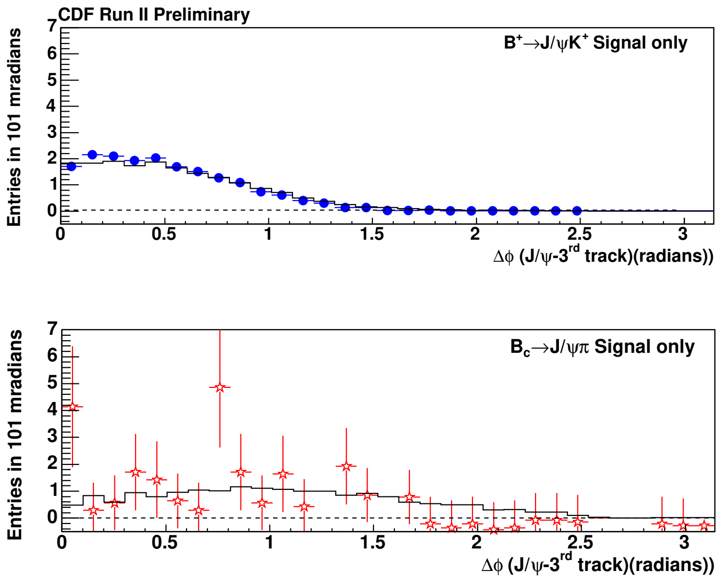

Figure 28: Angle in the $x - y$ plane between the direction of flight of the J/ψ and the pion track. Upper figure is for the B_u case, the lower figure is for theB_c case. is the same distribution for signal-only Monte Carlo sample. The B_c sample was generated with B_c mass M_{Bc} = 6.4 GeV/c^2 and $c\tau = 138\mu$m.

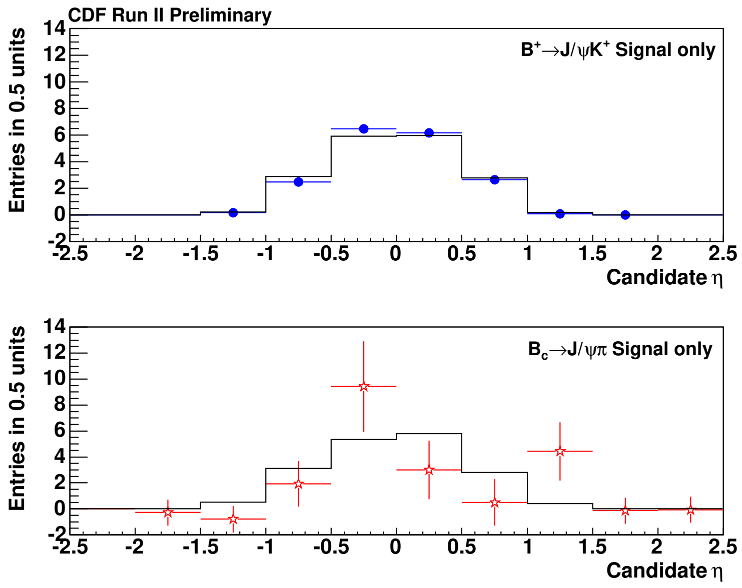

Figure 29: Pseudo-rapidity of the candidate. Upper plot: the distribution for the B_u signal, sideband subtracted. Lower plot: the same distribution for the signal events, sideband subtracted (data points). The solid-line histograms are the same distributions obtained from BGenerator Monte Carlo (signal-only sample). For B_c we used $M_{Bc} = 6.4$ GeV/c^2 and $c\tau = 138\mu$m.

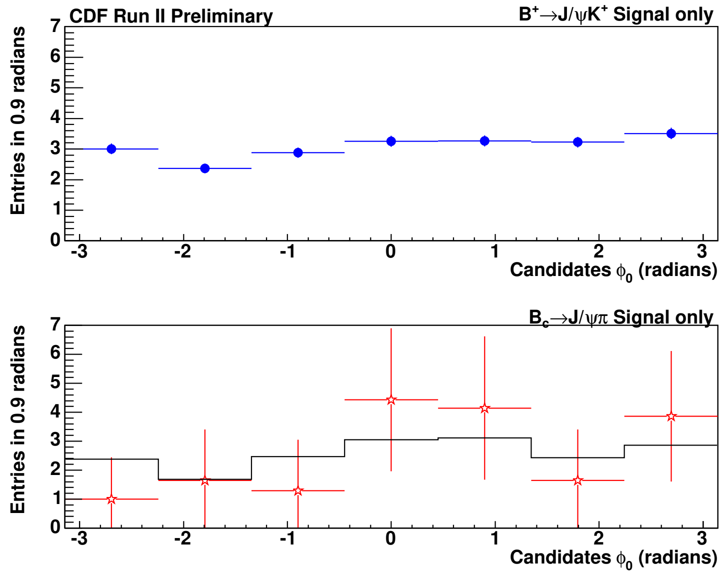

Figure 30: Distribution of the polar angle of the candidate. Upper plot: the distribution for the B_u signal, sideband subtracted, the lower plot shows the same distribution for the signal events, sideband subtracted (data points). The histogram in the lower plot is the same distribution for candidates from BGenerator Monte Carlo (signal-only sample), with mass = 6.4 GeV/c^2 and $c\tau = 138\mu$m.

$N_u = 4416 \pm 83$. The width of the gaussian is a measurement of the vertex resolution. For the LSB region we find 2252 ± 74 feed-down events, a narrow width $\sigma_1 = 25 \pm 3\mu$m (36% of the candidates) and a wide width $\sigma_2 = 78 \pm 6\mu$m.

We expect the same kind of excess in the case of B_c if the B_c signal is real, although with much reduced statistics.

9.2 The data sample $B_c \to J/\psi + track + X$

In the case of B_c the signal to background ratio is much lower and effect will be less spectacular than in fig. 32. However, an excess of tracks can still be expected with low impact parameter with respect to the J/ψ vertex.

As before, we define a signal region, an upper and a lower sideband. The lower sideband is defined as the region $5.600 < m_{J\psi\pi} < 6.187$ GeV/c^2. The lower bound is set to avoid the Λ_b mass region and the upper bound is set to about 100 MeV ($\approx$6-σ) from the signal peak. The upper side band is defined as the region with $6.387 < m_{J/\psi\pi} < 7.200$ GeV/c^2.

As shown in fig. 38, the B_c Monte Carlo simulation predicts no gap between the fully reconstructed signal and the partially reconstructed feed-down candidates. This is due to the presence of the semileptonic decays $B_c \to J/\psi l \nu_l$

In order to evaluate the expected number of feed-down candidates relative to the signal, we use BGenerator (signal-only) Monte Carlo, and we use EvtGen as decayer. All B_c decays are left open, the J/ψ's are forced to decay to two muons. We select only the events that pass the J/ψ trigger requirements. All the B_c decays for which there is a theoretical expectation [6] were included. The contribution from the exclusive decay $B_c \to J/\psi a_1^+$ is not included in this sample, but we generated it separately. We rescale its contribution by assuming a branching ratio that is four times larger than $B_c \to J/\psi\pi^+$. This is consistent with the corresponding branching ratio in the case of $B^+ \to D^{*0}a_1^+$ compared to $B^+ \to D^{*0}\pi^+$ [12]. Decays into χ_c are not included, owing to their unknown branching ratios. The B_c decay table for this MC sample is reported in appendix A. Because the decay table is incomplete, we expect that the Monte Carlo will give an approximate lower bound of the expected number of feed-down candidates.

Full detector and trigger simulation is used and the MC sample is analyzed in exactly the same way as the data, including trigger and analysis cuts. The L1 and L2 triggers are fully simulated, while the L3 off-line cuts are applied at the analysis level. As shown in fig. 37, the lower sideband extends for a width of 587 MeV, with the upper edge at 100 MeV below the signal peak, which in the Monte Carlo sample is at 6.400 GeV/c^2.

Using the relaxed cuts the number of signal events in the generic B_c Monte Carlo sample is $N_S = 51$ and the number of feed-down candidates is $N_{fd} = 175$. Using the analysis cuts for the full reconstructed mode we find 37 signal events and 112 feed-down events. Therefore, if the decay table and the p_T spectrum used in the Monte Carlo are correct, on rescaling to 37 signal events we expect 90 events in the feed-down region. The contribution of the $B_c \to J/\psi a_1^+$ has been calculated to be about 6 candidates, which makes a total of 96 expected events. As no Branching Ratio has been measured yet for this meson, a large uncertainty on such a contribution is unavoidable.

In the data we plot in fig. 39 the impact parameter distributions for the lower and upper sidebands showing that for large impact parameters the distributions have identical shape, but for small impact parameter values the lower sideband region has an excess. The difference between the lower and upper sideband *i.p.* distributions is plotted in fig. 40. We count an excess of about 200 candidates with $i.p. < 50\mu$m. In fig. 41 we superimpose the distribution observed for the B_u, rescaled, showing that the shape is compatible with the same distribution for the B_u. In this case, because of the smaller statistics, we use a single Gaussian to fit the *i.p.* distribution (fig. 42) and we fix the width to the value obtained in the case of the *i.p.* distribution for the B_u signal. This fit gives a total of 172 ± 49 events. Some alternative fits were used to assess a systematic error: by varying the width of the distribution within the statistical errors and using the parameters from the fits to the B_u signal or to the $B_{u,d}$ LSB a systematic uncertainty of ± 15 events is assigned to the fitted number of events. It is possible to suppose that the impact parameter difference between the lower and upper sidebands might simply reflect a mass-dependent variation on the combinatorial background distribution. To check this, the upper side band was divided into an upper and a lower region and the impact parameter distributions in these were compared. No evidence for any difference was found (fig. 43).

We conclude that the feed-down signal has been observed, giving confirmatory support to our interpretation of the observed peak in the $J/\psi\pi^+$ spectrum as a narrow B_c resonance. On the basis of the number of B_c signal events, the included decay channels in the Monte Carlo simulation imply an expectation of 96 ± 30 feed-down events. The observed number is somewhat larger but of the same order of magnitude. Since it is known that not all the decays were correctly included in the Monte Carlo, we consider the agreement to be reasonable, given the uncertainties in the model.

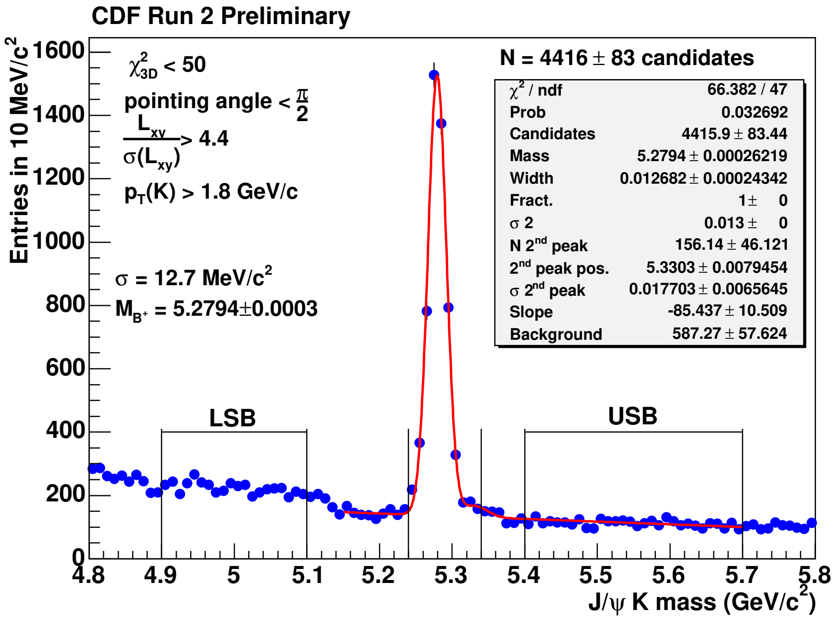

Figure 31: Mass spectrum of the $B_u^+ \to J/\psi K^+$, obtained with the relaxed cuts described in the text. The sideband regions that we have used in the analysis of the partially reconstructed decays are also indicated. We fit the distribution with one gaussian for the signal $B_u^+ \to J/\psi K^+$, one gaussian for the $B_u \to J/\psi\pi^+$ component and a linear background. We obtain 4416 ± 83 candidates.

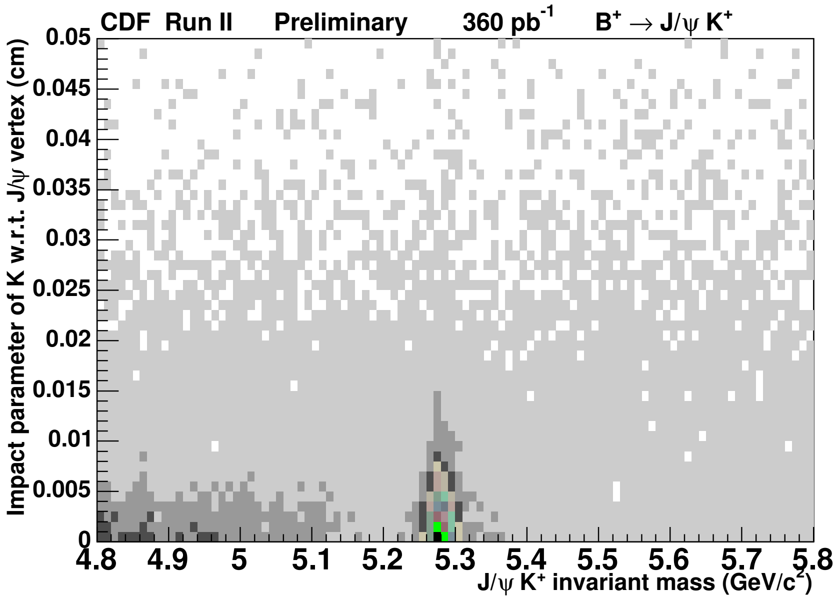

Figure 32: B_u case: Impact parameter of Kaon track with respect to the J/ψ vertex as a function of candidate mass: $\chi^2 < 50$ and $d_0(B) < 2$ mm, pointing angle $\beta < \pi/2$

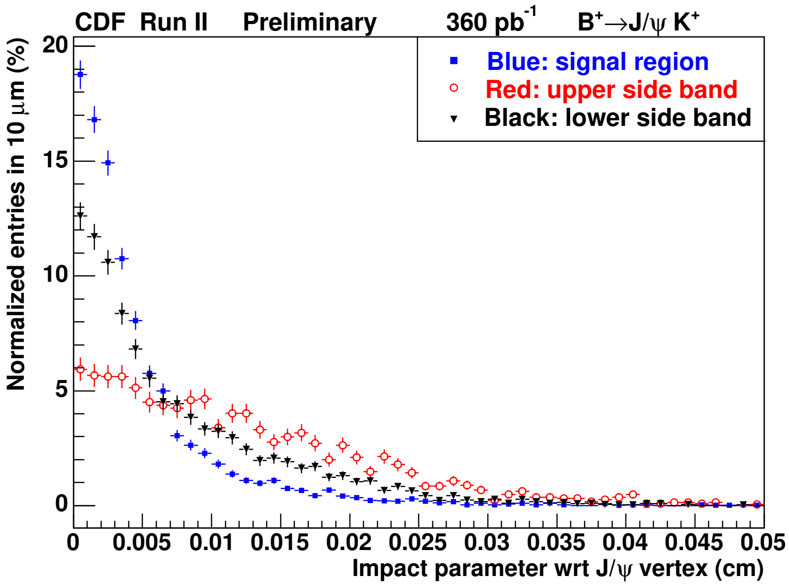

Figure 33: B_u case: impact parameter distribution of third track with respect to the J/ψ vertex for the three regions: upper side band, lower side band and signal. All distributions are normalized to the same area.

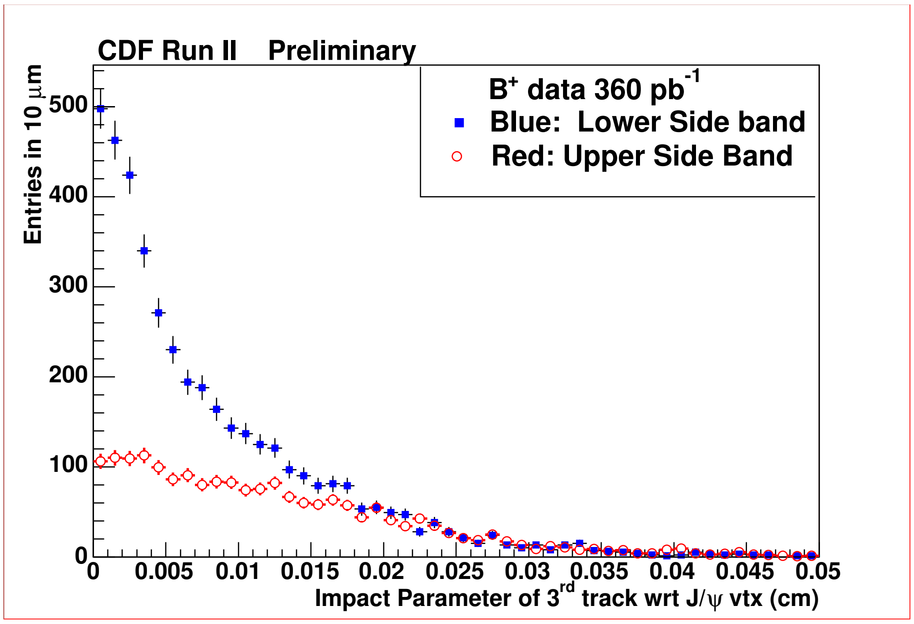

Figure 34: B_u case: impact parameter distribution of third track with respect to the J/ψ vertex for the upper side band and the lower side band. The distribution from the upper side band has been normalized to the same mass interval as the LSB.

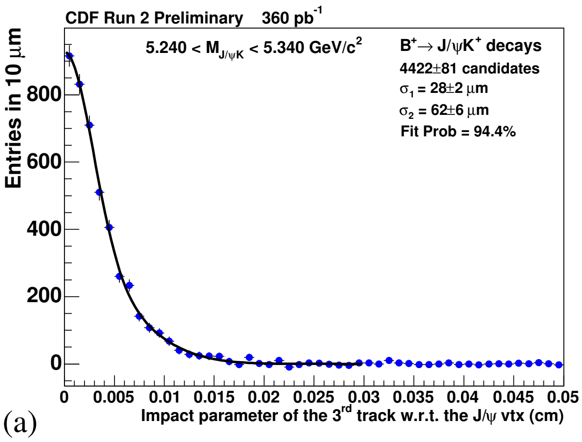

(a)

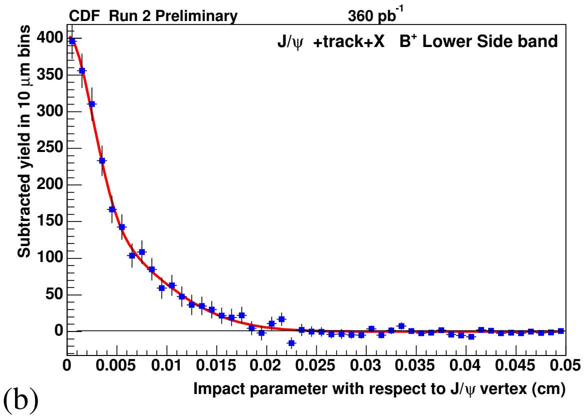

(b)

Figure 35: Excess distribution of the impact parameter of the third track with respect to the J/ψ vertex. (a) shows the the B_u signal over the Upper Side Band. A double gaussian fit yields 4422 ± 81 events, and width of $\sigma_1 = 28 \pm 2\mu$m and $\sigma_2 = 62 \pm 6\mu$m. (b) shows the B_u lower sideband over the upper side band, that shows an excess due to the partially reconstructed decays $B_{u,d} \to J/\psi + \mathit{track} + X$.

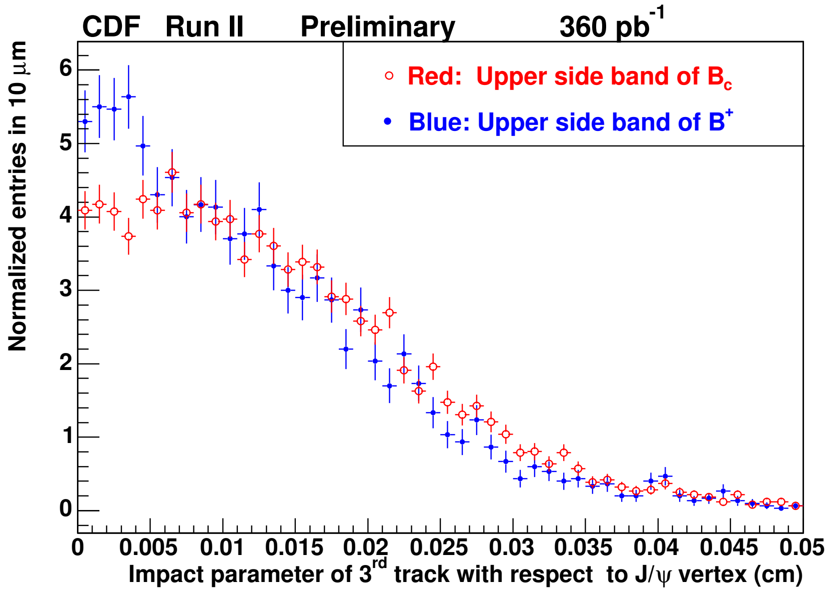

Figure 36: Comparison of the distributions of impact parameter of the third track with respect to the J/ψ vertex for the B_u Upper Side Band and for the Upper Side Band of the B_c. The two distributions are normalized to the same area. It should be noted that the upper side band region of the B_u is actually a lower side band for the B_c.

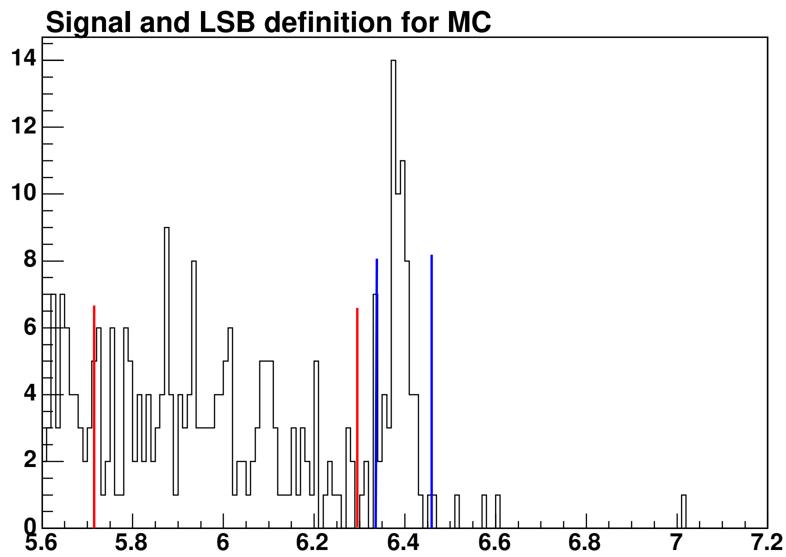

Figure 37: Mass plot with relaxed cuts, of a B_c Monte Carlo sample, where many decays of the $B_c \rightarrow J/\psi X$ are simulated and only 3-track vertices are reconstructed. We assumed $c\tau = 138\mu$m and M(B_c) = 6.4 GeV/c^2. The signal region and LSB are also shown. We have 175 entries in LSB and 63 signal events.

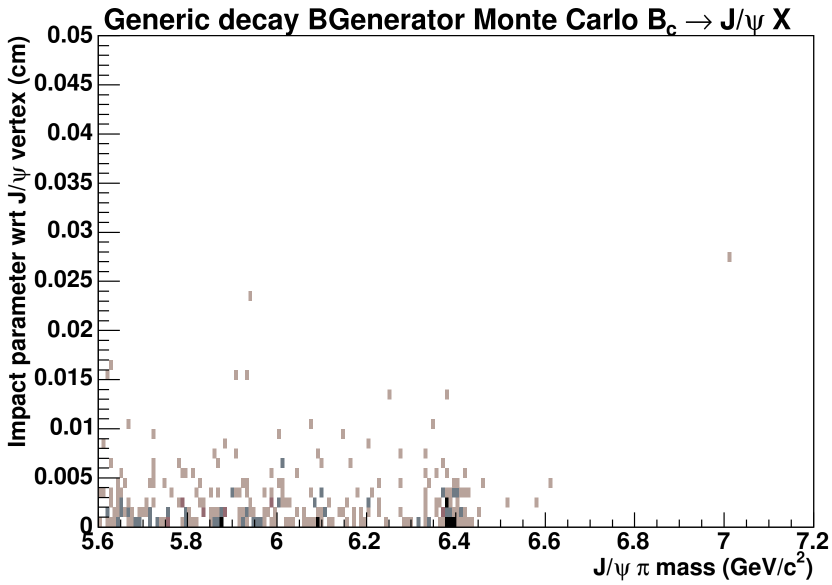

Figure 38: Monte Carlo B_c: Impact parameter of pion track with respect to the J/ψ vertex as a function of candidate mass for the generic BGenerator Monte Carlo sample with B_c decaying in all channels included in EvtGen decay table release 5.3.3. No $J/\psi\ a_1$ contribution, nor hadronic decays to excited charmonium.

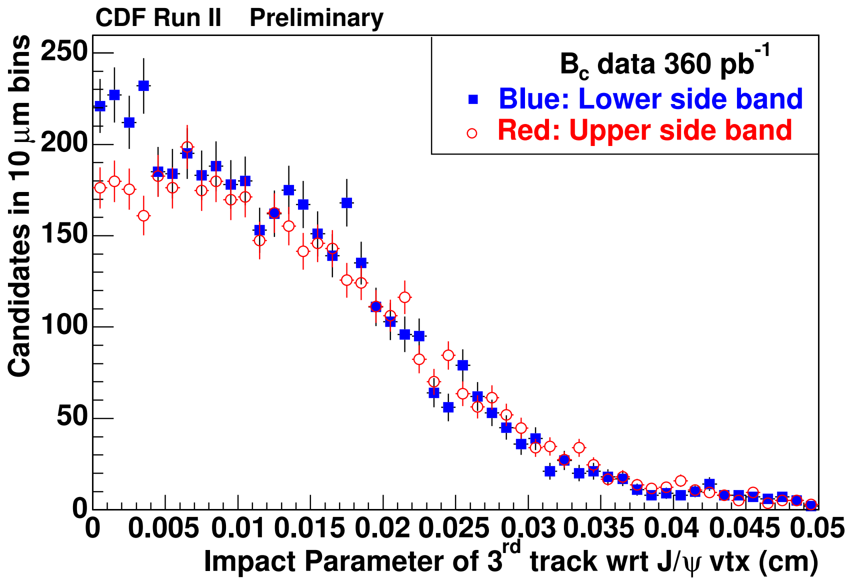

Figure 39: Distributions of the impact parameter of the third track in the lower side band (squares) and in the upper side band (circles) with respect to the B_c signal peak. The USB distribution is normalized to the same mass interval as the LSB. The excess at low impact parameter is visible.

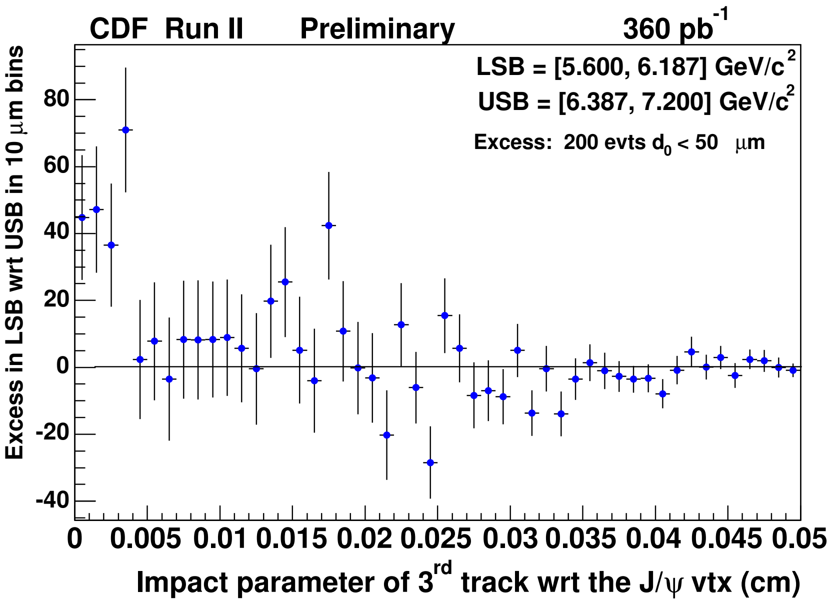

Figure 40: In the B_c case the difference of the distribution of the impact parameter of the third track with respect to the J/ψ vertex between the Lower Side Band and the Upper Side Band (properly normalized) shows an excess of about 200 events in the first region (impact parameter $< 50\mu$m).

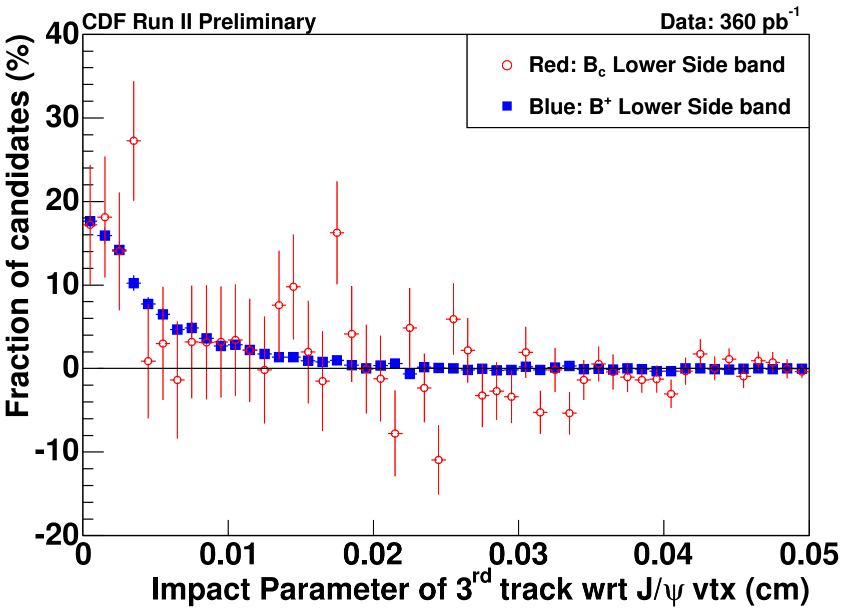

Figure 41: Comparison of the distributions of impact parameter of the third track with respect to the J/ψ vertex for the B_u Lower Side Band and for the B_c Lower Side Band. In each case the normalized distribution from the respective upper side band has been subtracted. The two distributions shown are normalized to the same area.

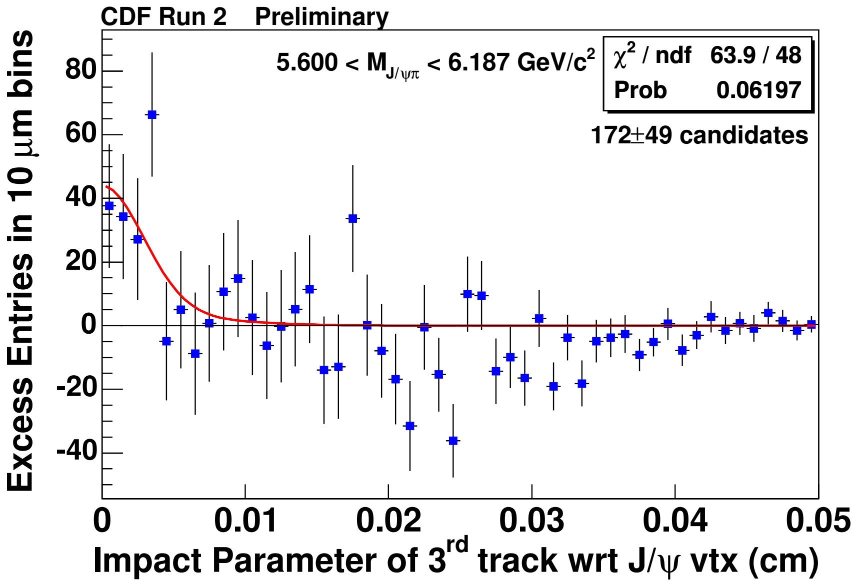

Figure 42: Excess distribution of the impact parameter of the third track with respect to the J/ψ vertex for the B_c Lower Side Band over the Upper Side Band of the B_c. A gaussian fit yields 172 ± 49 events, with width fixed from fit in the B_u case.

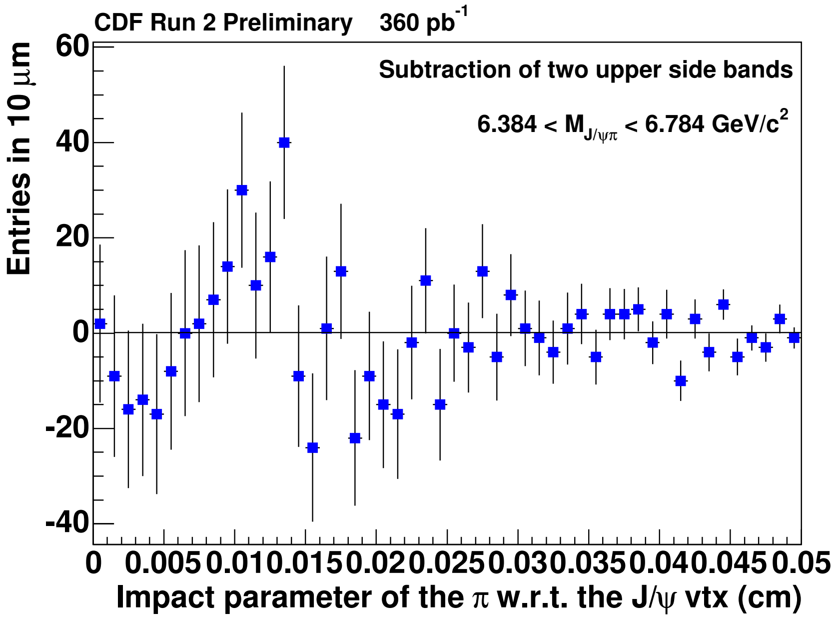

Figure 43: The Upper Side Band of the B_c has been divided in two bands. The distribution of the impact parameter of the third track with respect to the J/ψ vertex for candidates in the the upper half of the USB is subtracted from the same distribution for the lower half of the upper side band. No excess of events at low impact parameter is observed in this case.

10 Conclusions

- A variety of checks on the B_c candidates have been performed, making comparisons between these candidates and expectations from Monte Carlo and from the B_u control sample. No statistically significant discrepancies have been seen.

- An investigation of the partially reconstructed feed-down events was performed by considering the impact parameter of the third track with respect to the J/ψ. The B_c data exhibit behavior similar to B_u, but with a much relative higher level of combinatoric background. There is a significant peak for invariant masses below the B_c (6287 MeV/c^2), and a smooth background shape for the high mass combinatoric events. The subtracted peak in $J/\psi\ \pi^+$ agrees well with the same peak for J/ψ K$^+$, as would be expected assuming the same resolution on the impact parameter with respect to the J/ψ vertex position in x, y.

Acknowledgments

We are grateful the godparents Barry Wicklund, Steve Levy and Stephanie Menzemer, as well as to Matthew Herndon, Tom LeCompte, Stefano Giagu, Marco Rescigno, Rolf Oldeman and Giovanni Punzi for useful discussions and suggestions.

Appendix A

Decay table for the package EvtGen used in the generic B_c Monte Carlo sample. This decat table is the default in the CDF software release 5.3.3 The decays to $J/\psi\ a_1^+$ are generated separately.

```
Decay B_c-
0.01600    tau-       anti-nu_tau               SLN;
#
#                 SemiLeptonic Decays
0.01900    J/psi      e-      anti-nu_e         PHOTOS  PHSP;
0.00094    psi(2S)    e-      anti-nu_e         PHOTOS  PHSP;
0.00750    eta_c      e-      anti-nu_e         PHOTOS  PHSP;
0.00020    eta_c(2S)  e-      anti-nu_e         PHOTOS  PHSP;
0.00004    anti-D0    e-      anti-nu_e         PHOTOS  PHSP;
0.00018    anti-D*0   e-      anti-nu_e         PHOTOS  PHSP;
0.04030    anti-B_s0  e-      anti-nu_e         PHOTOS  PHSP;
0.05060    anti-B_s*0 e-      anti-nu_e         PHOTOS  PHSP;
0.00340    anti-B0    e-      anti-nu_e         PHOTOS  PHSP;
0.00580    anti-B*0   e-      anti-nu_e         PHOTOS  PHSP;
#
0.01900    J/psi      mu-     anti-nu_mu        PHOTOS  PHSP;
0.00094    psi(2S)    mu-     anti-nu_mu        PHOTOS  PHSP;
0.00750    eta_c      mu-     anti-nu_mu        PHOTOS  PHSP;
0.00020    eta_c(2S)  mu-     anti-nu_mu        PHOTOS  PHSP;
0.00004    anti-D0    mu-     anti-nu_mu        PHOTOS  PHSP;
0.00018    anti-D*0   mu-     anti-nu_mu        PHOTOS  PHSP;
0.04030    anti-B_s0  mu-     anti-nu_mu        PHOTOS  PHSP;
0.05060    anti-B_s*0 mu-     anti-nu_mu        PHOTOS  PHSP;
0.00340    anti-B0    mu-     anti-nu_mu        PHOTOS  PHSP;
0.00580    anti-B*0   mu-     anti-nu_mu        PHOTOS  PHSP;
#
0.00480    J/psi      tau-    anti-nu_tau               PHSP;
0.00008    psi(2S)    tau-    anti-nu_tau               PHSP;
0.00230    eta_c      tau-    anti-nu_tau               PHSP;
0.000016   eta_c(2S)  tau-    anti-nu_tau               PHSP;
0.00002    anti-D0    tau-    anti-nu_tau               PHSP;
0.00008    anti-D*0   tau-    anti-nu_tau               PHSP;
#
#
#                 Hadronic Decays
0.00200    eta_c      pi-     PHSP;
0.00420    rho-       eta_c   SVS;
0.00013    eta_c      K-      PHSP;
0.00020    K*-        eta_c   SVS;
0.00130    J/psi      pi-     SVS;
```

```
0.00400    J/psi      rho-     SVV_HELAMP 1.0 0.0 1.0 0.0 1.0 0.0;
0.00011    J/psi      K-       SVS;
0.00022    J/psi      K*-      SVV_HELAMP 1.0 0.0 1.0 0.0 1.0 0.0;
#
0.000053   D-         D0       PHSP;
0.000075   D*0        D-       SVS;
0.000049   D*-        D0       SVS;
0.00033    D*-        D*0      SVV_HELAMP 1.0 0.0 1.0 0.0 1.0 0.0;
0.0000048  D_s-       D0       PHSP;
0.0000071  D*0        D_s-     SVS;
0.0000045  D_s*-      D0       SVS;
0.000026   D_s*-      D*0      SVV_HELAMP 1.0 0.0 1.0 0.0 1.0 0.0;
#
0.0000003  D-         anti-D   PHSP;
0.0000003  anti-D*0   D-       SVS;
0.0000004  D*-        anti-D   SVS;
0.0000016  anti-D*0   D*-      SVV_HELAMP 1.0 0.0 1.0 0.0 1.0 0.0;
0.0000066  D_s-       anti-D   PHSP;
0.0000063  anti-D*0   D_s-     SVS;
0.0000085  D_s*-      anti-D   SVS;
0.0000404  D_s*-      anti-D   SVV_HELAMP 1.0 0.0 1.0 0.0 1.0 0.0;
#
0.00280    eta_c      D_s-     PHSP;
0.00270    D_s*-      eta_c    SVS;
0.00015    eta_c      D-       PHSP;
0.00010    D*-        eta_c    SVS;
0.00170    J/psi      D_s-     SVS;
0.00670    J/psi      D_s*-    SVV_HELAMP 1.0 0.0 1.0 0.0 1.0 0.0;
0.00009    J/psi      D-       SVS;
0.00028    J/psi      D*-      SVV_HELAMP 1.0 0.0 1.0 0.0 1.0 0.0;
#
0.16400    anti-B_s0  pi-      PHSP;
0.07200    rho-       anti-B   SVS;
0.01060    anti-B_s0  K-       PHSP;
0.00000    K*-        anti-B   SVS;
0.06500    anti-B_s*0 pi-      SVS;
0.20200    anti-B_s*0 rho-     SVV_HELAMP 1.0 0.0 1.0 0.0 1.0 0.0;
0.00370    anti-B_s*0 K-       SVS;
0.00000    anti-B_s*0 K*-      SVV_HELAMP 1.0 0.0 1.0 0.0 1.0 0.0;
0.01060    anti-B0    pi-      PHSP;
0.00960    rho-       anti-B   SVS;
0.00070    anti-B0    K-       PHSP;
0.00015    K*-        anti-B   SVS;
0.00950    anti-B*0   pi-      SVS;
0.02570    anti-B*0   rho-     SVV_HELAMP 1.0 0.0 1.0 0.0 1.0 0.0;
```

```
0.00055    anti-B*0   K-       SVS;
0.00058    anti-B*0   K*-      SVV_HELAMP 1.0 0.0 1.0 0.0 1.0 0.0;
0.00037    B-         pi0      PHSP;
0.00034    rho0       B-       SVS;
0.01980    B-         K0       PHSP;
0.00430    K*0        B-       SVS;
0.00033    B*-        pi0      SVS;
0.00090    B*-        rho0     SVV_HELAMP 1.0 0.0 1.0 0.0 1.0 0.0;
0.01600    B*-        K0       SVS;
0.01670    B*-        K*0      SVV_HELAMP 1.0 0.0 1.0 0.0 1.0 0.0;
#
0.0200235  cs_0       anti-uu_0         JETSET 23;
0.0400470  cs_1       anti-uu_1         JETSET 23;
#
Enddecay
```

References

[1] CDF/DOC/BOTTOM/CDFR/6873 (2004), J. Cranshaw, V. Papadimitriou, M. Spezziga: *Blind analysis proposal for* $B_c \to J/\psi\pi$.

[2] CDF note 7018 (2004), P. Bussey, S. D'Auria, L. Nicolas, V. Papadimitriou, M. Spezziga: *Search of a* $B_c \to J/\psi\pi$ *signal: Monte Carlo Validation.*

[3] CDF note 7133 (2004), P. Bussey, S. D'Auria, L. Nicolas, V. Papadimitriou, M. Spezziga: *Search for a Bc to* J/ψ *signal: cuts optimization* .

[4] CDF note 7282 (2004), P. Bussey, S. D'Auria, L. Nicolas, V. Papadimitriou, M. Spezziga: *Optimization of cuts for Bc to* J/ψ *search* .

[5] CDF Collaboration, Phys. Rev. D58 112004 (1998).

[6] V. V. Kiselev, hep-ph/0308214.

[7] PHYSTAT2003 arXiv:physics/0308063, G. Punzi: *Sensitivity of searches for new signals and its optimization.*.

[8] CDF/PHYS/BOTTOM/6905, M. Campanelli, E. Gerchtein: *Calibration of the momentum scale for Kalman refitter using* J/ψ *events.*

[9] Chao Hsi Chang: arXiv:hep-ph/0309121.

[10] A. V. Berezhnoy, Private communication, calculation based on the SIMUB simulation package.

[11] For a detailed scrutiny of the background encountered in a preliminary Run I analysis, see A. B. Wicklund, CDF/DOC/BOTTOM/CDFR/5002 (1999)

[12] Eidelman et al., Physics Letters B 592 1-4 (2004) (particle data book 2004).

[13] CDF/DOC/BOTTOM/CDFR/6355, G. Bauer, A. Korn, C. Paus: *Update on Calibration of Energy Loss and Magnetic Field using* J/ψ *Events in Run II.*

[14] CDF/ANAL/BOTTOM/CDFR/6426, A. Korn, Ch. Paus, D. Starret al.: *Update on the Measurement of B Meson Masses in the Exclusive* J/ψ *Channels.*

[15] CDF/ANAL/BOTTOM/CDFR/6963, A. Korn, C. Paus: *Measurement of the B Hadron Masses in exclusive* J/ψ *Decay Channels.*

[16] W.A. Rolke, A.M. Lopez, PHYSTAT2003 and hep-ph/0206139.